2021 CESM Paleoclimate Workgin Group Meeting

Multi-scale climate variability during the Holocene:

A new group of simulations based on CESM

Liang Ning[1,2,3,4], Jian Liu[1,2], Zhengyu Liu[5], Mi Yan[1,2], Weiyi Sun[1], Lingfeng Wan[1], Kefan Chen[1], Chunhan Jin[1], et al.

1. Key Laboratory for Virtual Geographic Environment, Ministry of Education; State Key Laboratory Cultivation Base of Geographical Environment Evolution of Jiangsu Province; Jiangsu Center for Collaborative Innovation in Geographical Information Resource Development and Application；School of Geography, Nanjing Normal University, Nanjing 210023
2. Open Studio for the Simulation of Ocean-Climate-Isotope, Qingdao National Laboratory for Marine Science and Technology, Qingdao 266237
3. Climate System Research Center, Department of Geosciences, University of Massachusetts, Amherst, 01003, United States
4. State Key Laboratory of Loess and Quaternary Geology, Institute of Earth Environment, CAS
5. Department of Geography, The Ohio State University, Columbus, OH 43210, USA

2021.02.08

Outline

- Motivation
- NNU-Holocene and NNU-2ka Experimental designs
- Influences and mechanisms from natural and anthropogenic forcings on multi-scale climate variability during the Holocene
- Concluding remarks

Motivation

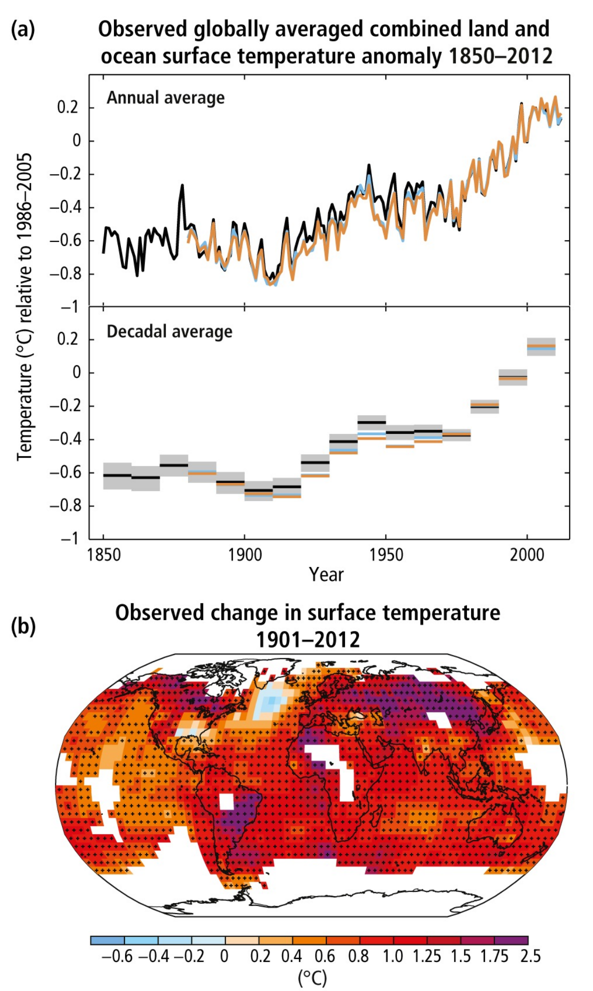

Global mean temperature has raised about 1°C since 1880s.

(IPCC AR5)

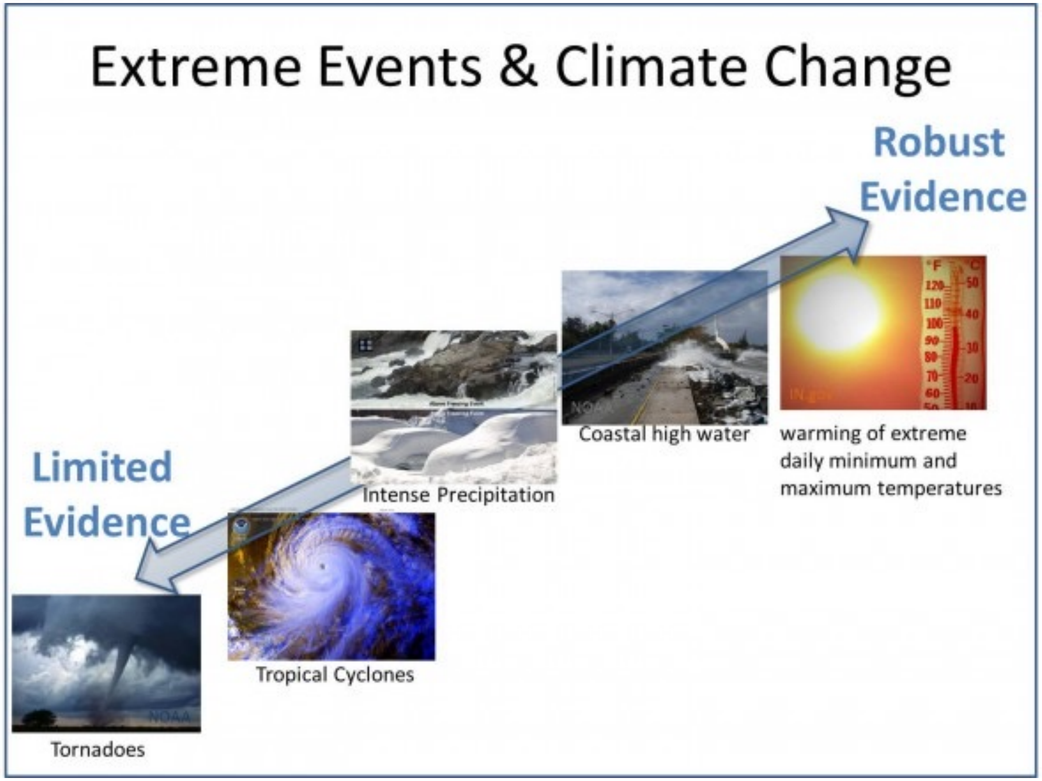

This temperature increase has resulted in substantial increases of flooding, droughts, heat wave, and other extreme climate events.

Motivation

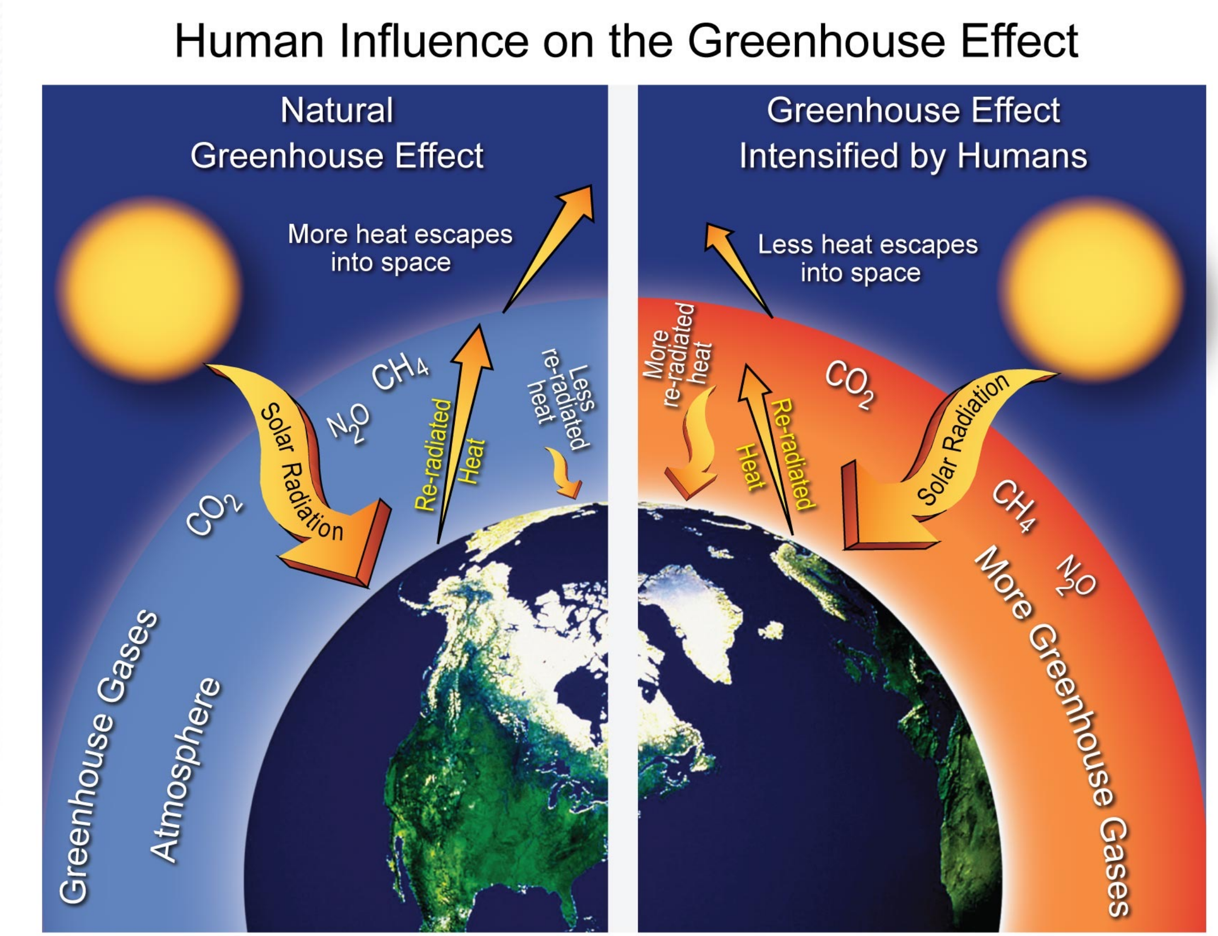

Source: internet

Usually, the current warming is attributed to the increases of greenhouse gases concentrations due to anthropogenic CO_2 emission.

Motivation

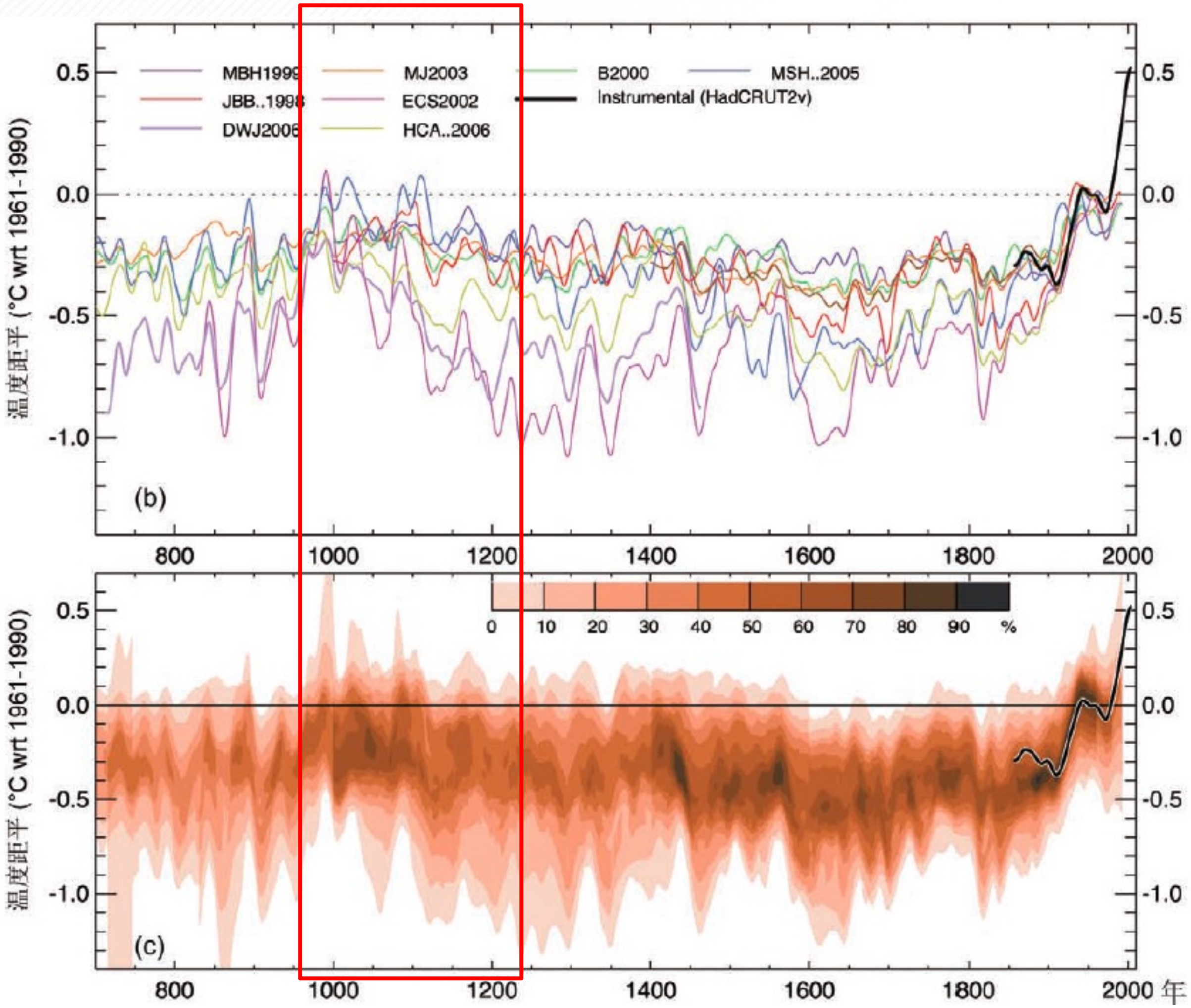

However, if looking back to the paleoclimate, there were similar warming periods during the history, e.g., Medieval Climate Anomaly (MCA), caused by natural forcing.

（Ge et al.，2013）

Motivation

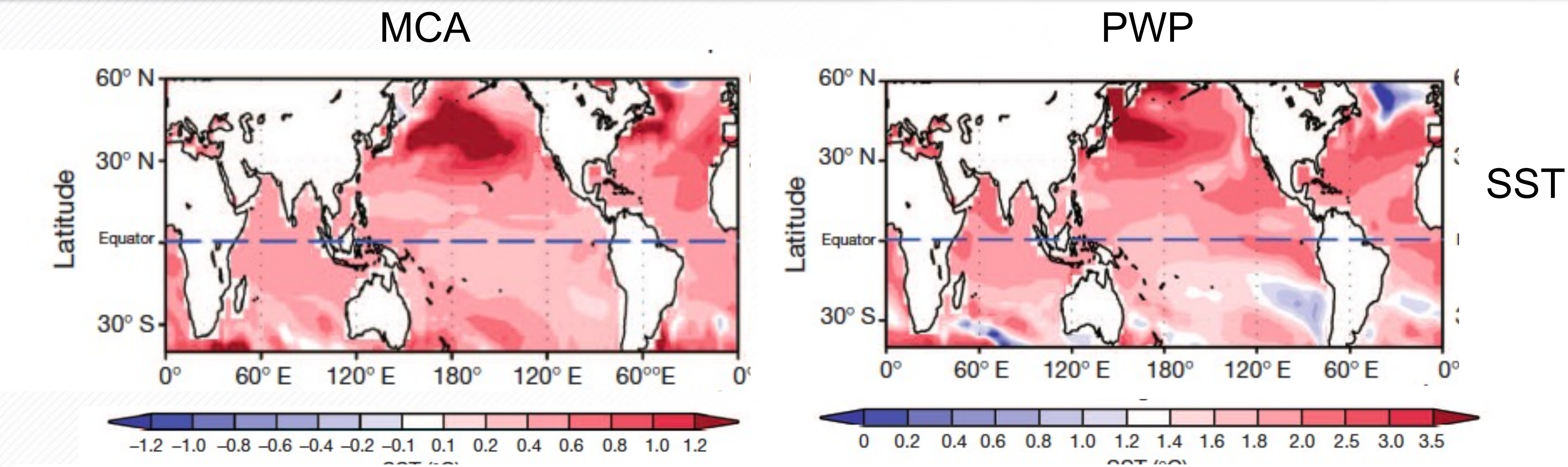

Question 1: How to differentiate the influences from natural forcings and anthropogenic forcings?

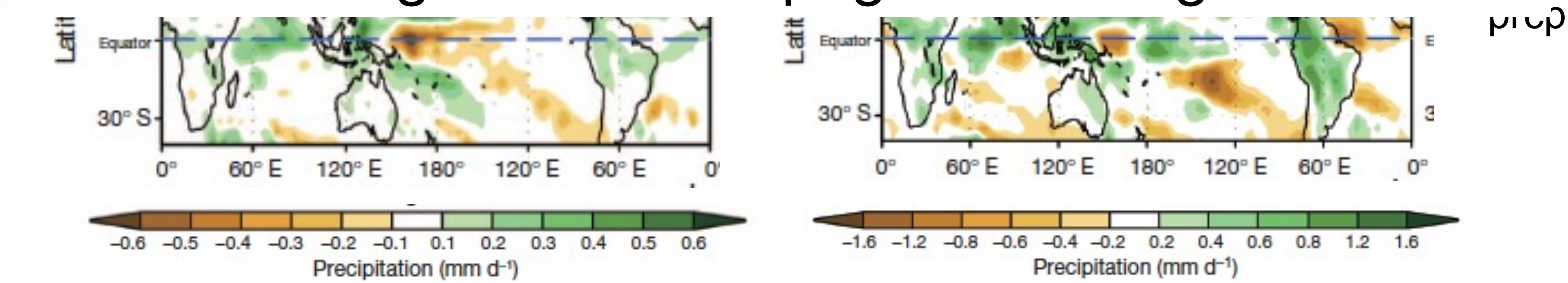

These warming periods during the pre-industrial periods are caused by natural forcing. Their spatial patterns are different from the present warming period, indicating different influences on global climate from natural and anthropogenic forcings. (Liu et al., 2013, *Nature*)

Motivation

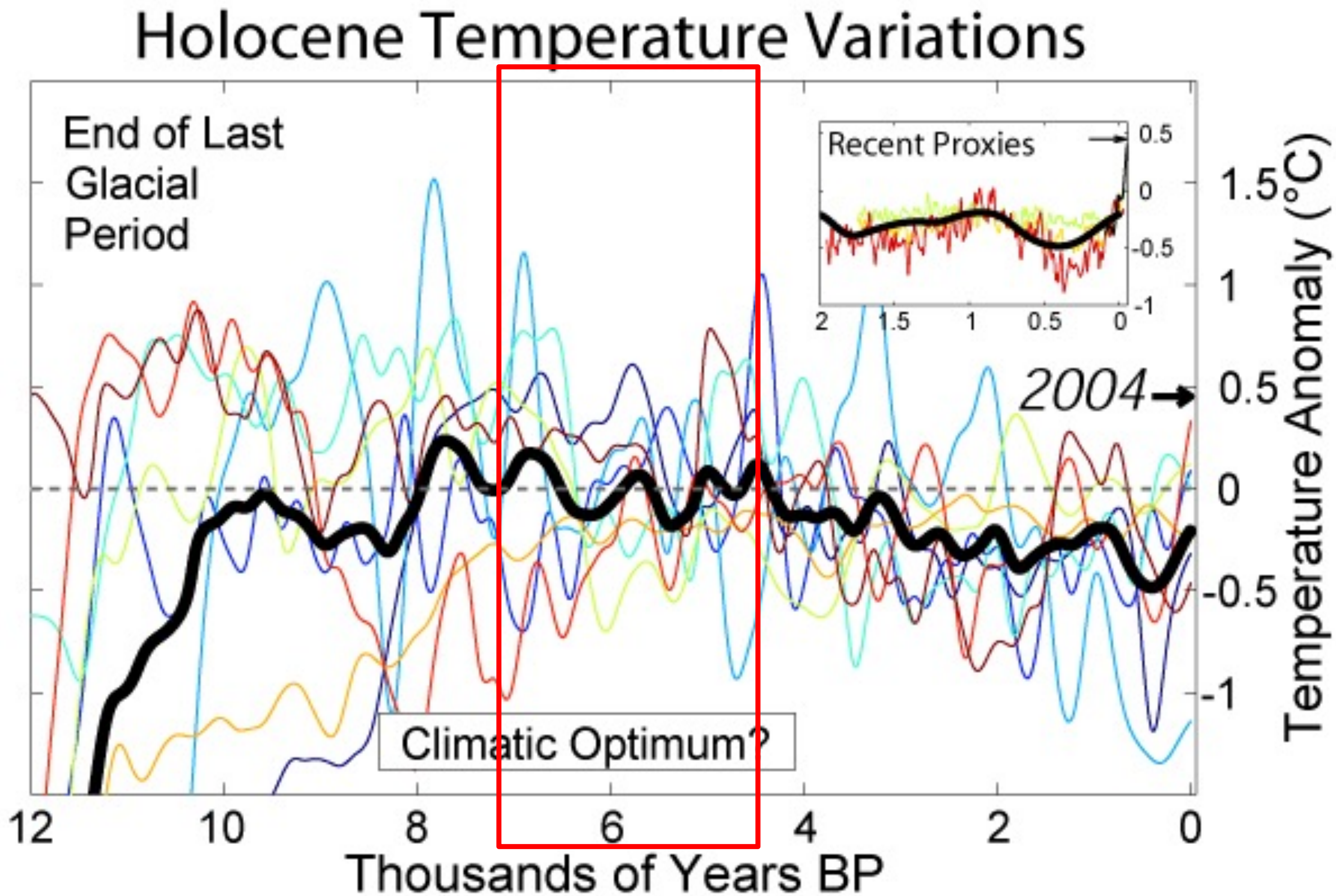

wikipedia

During the Holocene, there was also a millennial-scale warming period, i.e., the Holocene Thermal Maximum (also called Holocene Climate Optimum) between 7 to 4.2 ka BP (Wanner et al., 2011).

Motivation

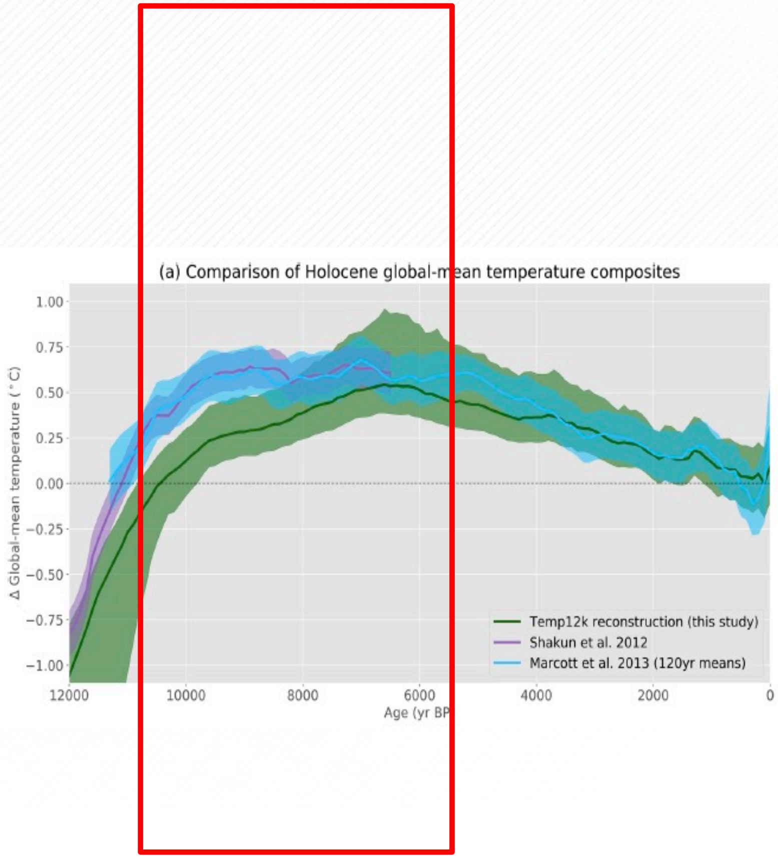

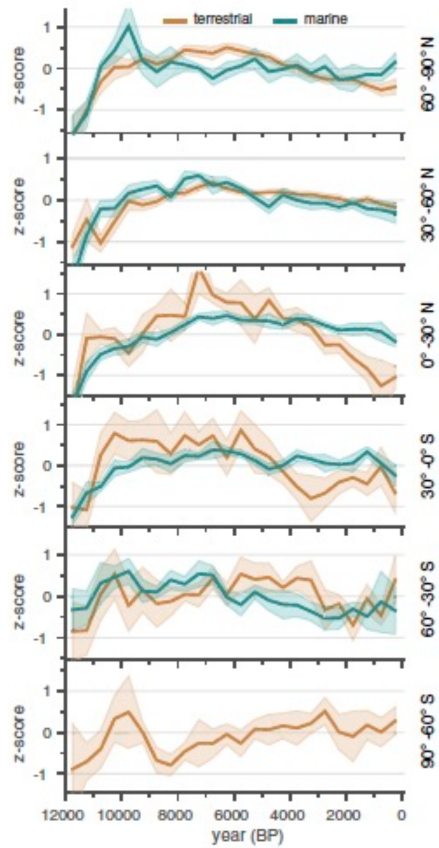

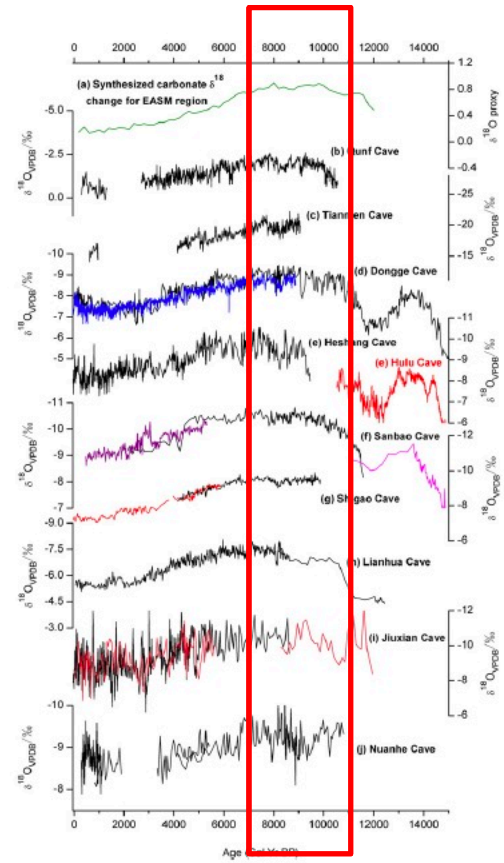

(Kaufman, 2020a&b)

(Liu et al., 2015)

However, different reconstructions do not agree with the timing of the Holocene Climate Optimum.

Motivation

Holocene conundrum?

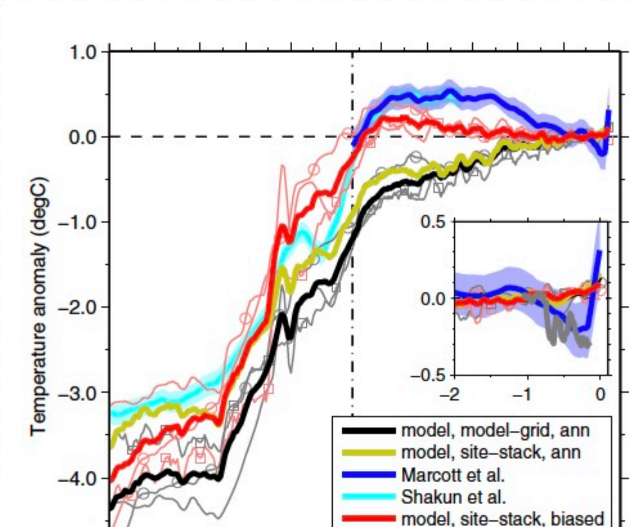

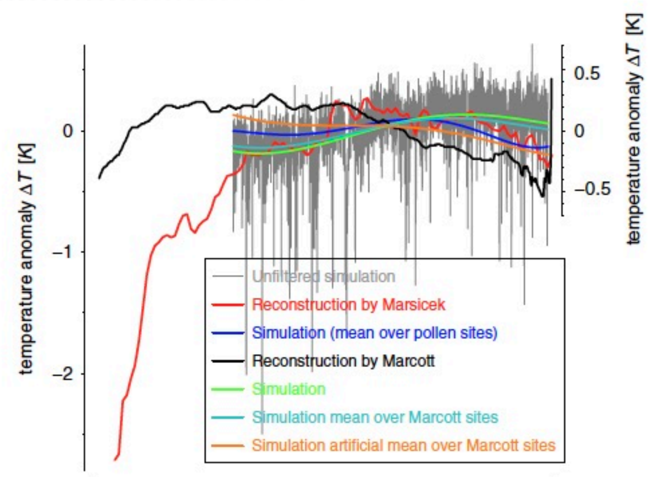

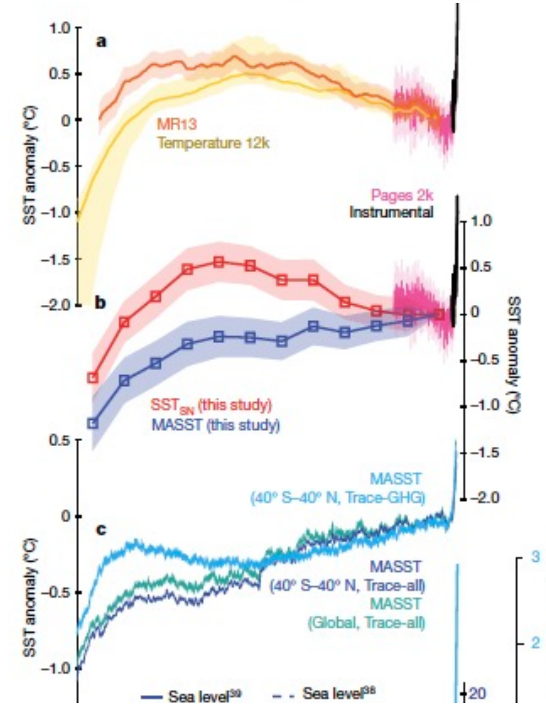

Question 2: When is the Holocene Climate Optimum? What are the contributions from different external forcings?

(Bova et al., 2021)

Models simulate increasing trends of annual temperature through the Holocene driven by the retreating of ice sheets and rising GHGs.

Motivation

“Bond cycle/events”

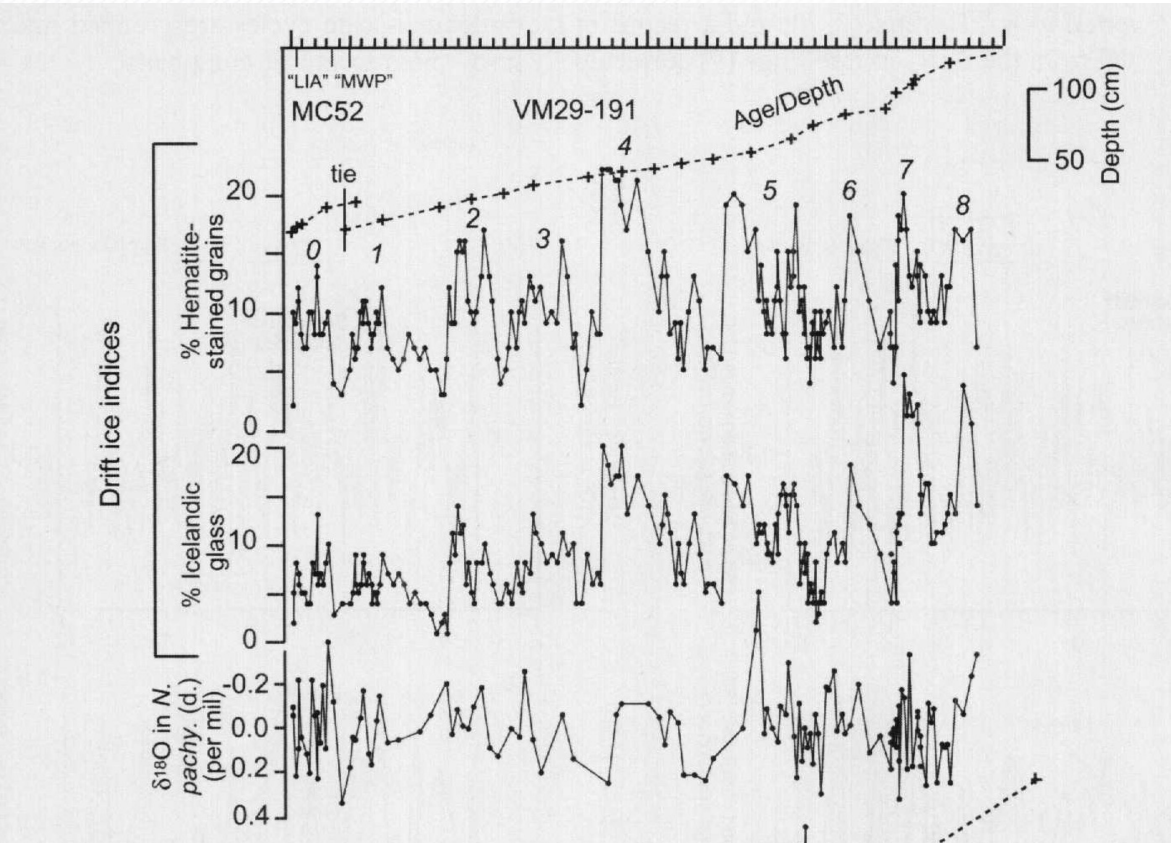

(Bond et al., 2001, *Science*)

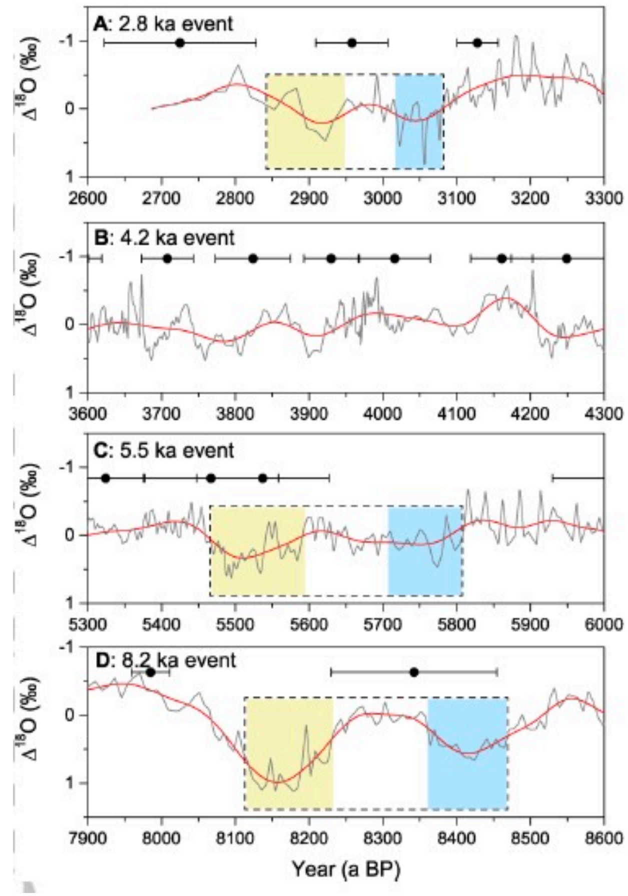

(Tan et al., 2021, *GRL*)

Question 3: What are the mechanisms behind the Bond Events?

Experimental design

- **Two groups of experiments**
  - NNU-Holocene
  - NNU-2ka
- **Model: Community Earth System Model (CESM)**
  - Developed by NCAR
  - Including models of Atmosphere, Ocean, Ice, Land surface, Carbon cycle, etc.
- **Seven/eight experiments in NNU-Holocene/NNU-2ka**
  - One control experiment
  - Five/six single-forcing sensitivity experiments
  - One all-forcing experiment

(Wang et al., 2015; Wan et al., 2020)

NNU-Holocene experimental design

NO	Name	External forcing	Integration time (year)
1	Control experiment (ctrl_B1850CN)	E=0.019419;Oblic = 24.227;Prec = -0.01763;TSI=1360.89 w/m2 CO_2=265 ppm;CH_4=660 ppb;N_2O=265 ppb	12000
2	Orbital parameter sensitivity experiment (orbit_B1850CN)	A. Berger,et al., 1997	12000
3	TSI sensitivity experiment (TSI_B1850CN)	L. E. A. Vieira et al., 2011	12000
4	GHGs sensitivity experiment (GHG_B1850CN)	CO_2: Luthi, D. et al., 2008. N_2O: Schilt, A. et al., 2010. CH_4: Loulergue, L. et al., 2008.	12000
5	LUCC sensitivity experiment (LUCC_B1850CN)	HYDE3.2 (Klein Goldewijk et al., 2011)	12000
6	Volcanic eruption sensitivity experiment (VOL_B1850CN)	Gao, C. et al., 2017	12000
7	All forcing experiment	Orbital+TSI+GHGs+LUCC+Vol	12000

(Wan et al., 2020, *Quaternary Sciences*)

NNU-Holocene experimental design

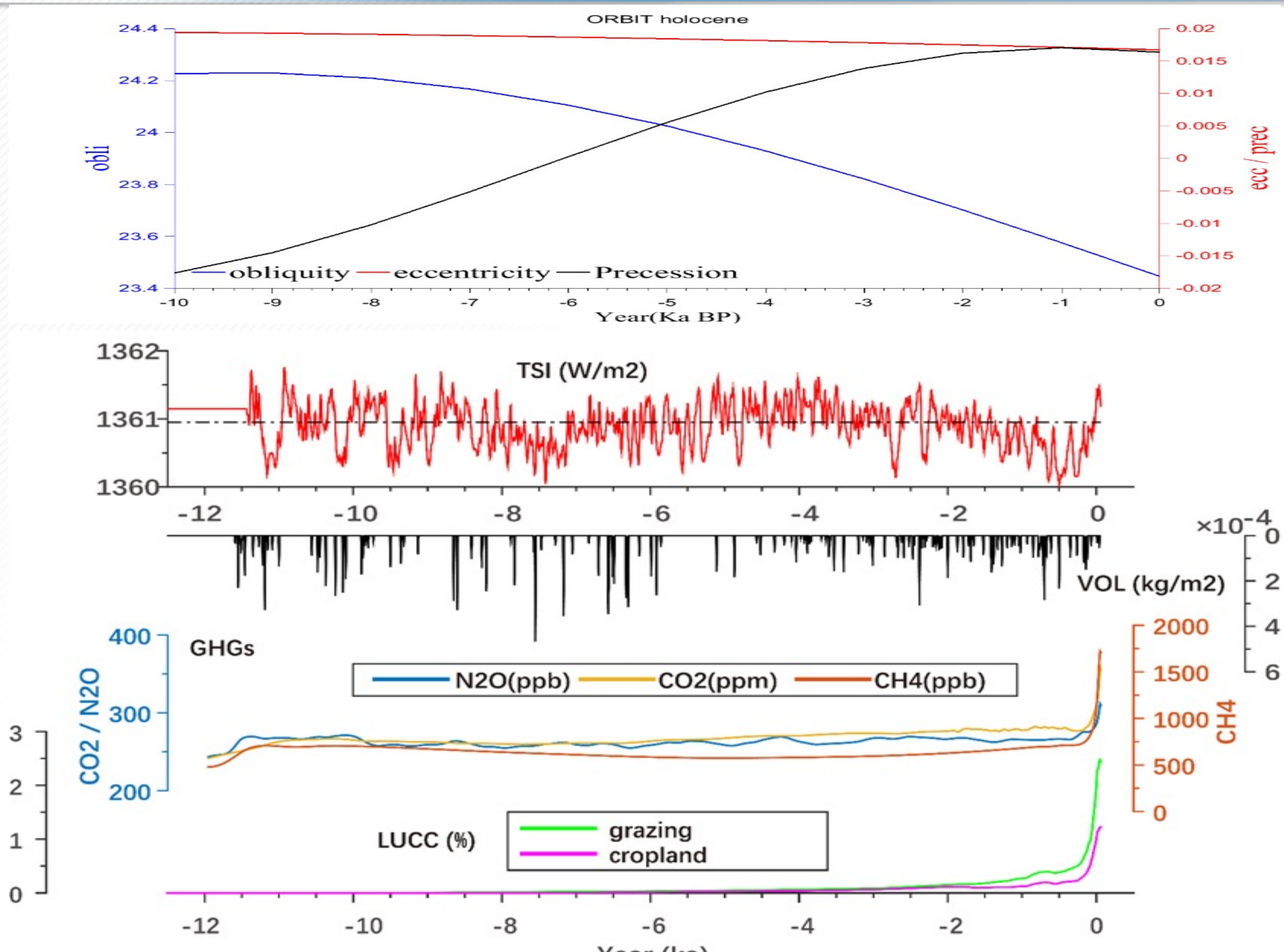

The ORB，TSI，VOL，GHGs, and LUCC forcings used in the NNU-Holocene experiment

(Wan et al., 2020, *Quaternary Sciences*)

NNU-2ka Experimental design

No	Name	External forcing	Simulation period (year)
1	Control experiment	NCAR 1850 A.D. external forcing	2400
2	TSI sensitivity experiment	Shipro et al., 2011	2000
3	Volcanic eruption sensitivity experiment	Gao et al., 2008	2000
4	GHGs sensitivity experiment	MacFailing et al., 2006	2000
5	LUCC sensitivity experiment	Kaplan et al., 2009	2000
6	Natural forcing sensitivity experiment	TSI+Vol	2000
7	Anthropogenic forcing sensitivity experiment	GHGs+LUCC	2000
8	All forcing experiment	TSI+Vol+GHGs+LUCC	2000

(Wang et al., 2015)

NNU-2ka Experimental design

External forcings

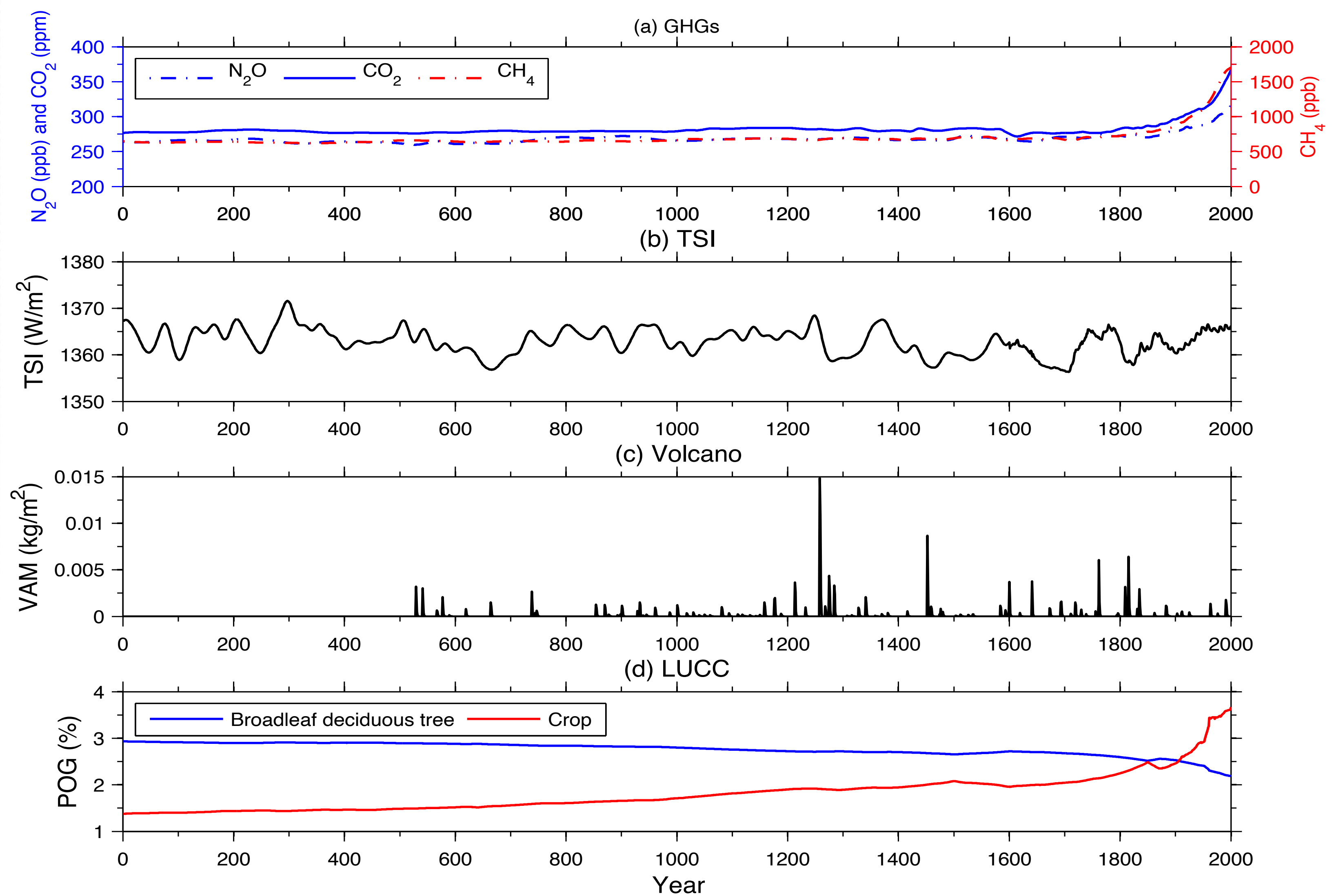

(Wang et al., 2015)

Applications of NNU-Holocene and NNU-2ka

- Based on NNU-Holocene and NNU-2ka, and TraCE-21ka, CESM-LME, and PMIP3 archives, etc., influences and mechanisms from natural and anthropogenic forcings on multi-scale climate variability during the Holocene were investigated:
  - Result 1: Millennial scale climate responses to external forcings in NNU-Holocene
  - Result 2: Mechanisms behind the 4.2 ka BP event
  - Result 3: Mechanisms of decadal megadroughts over eastern China
  - Result 4: Centennial to decadal climate responses to LUCC
  - Result 5: Influences of TSI on decadal EAM variability
  - Result 6: Influences from volcanic eruptions on ENSO and monsoon

Millennial scale

Centennial scale

Decadal scale

Interannual Scale

Result 1: Millennial scale climate responses to external forcings in NNU-Holocene

1. Simulation of Northern Hemisphere mid-latitude precipitation response to different external forcings during the Holocene

Reconstruction | **TraCE-21k** | **NNU-Holocene**

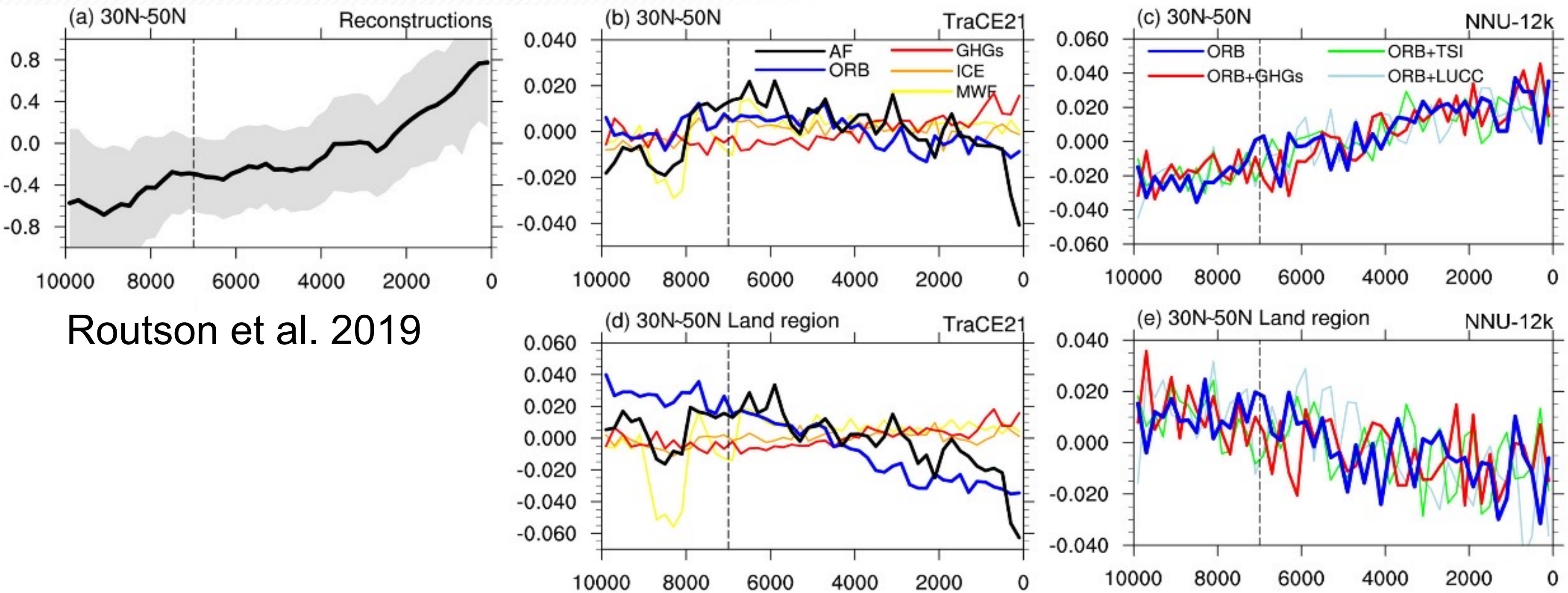

Routson et al. 2019

Northern Hemisphere mid-latitude (30°N-50°N) precipitation change

1) During 10-7 ka B.P., an increasing trend occurs in the TraCE21 **ICE**, **MWF** and **ORB** experiments.
2) In 7-0 ka, an increasing trend occurs in NNU-Holocene **ORB** experiment, which is consistent with the reconstructions, but the trend is concentrated in **marine areas**.

(Sun et al. 2020, *Quaternary Sciences*)

Eurasia land precipitation | **North American land precipitation**

Reconstruction

TraCE-21k

NNU-Holocene

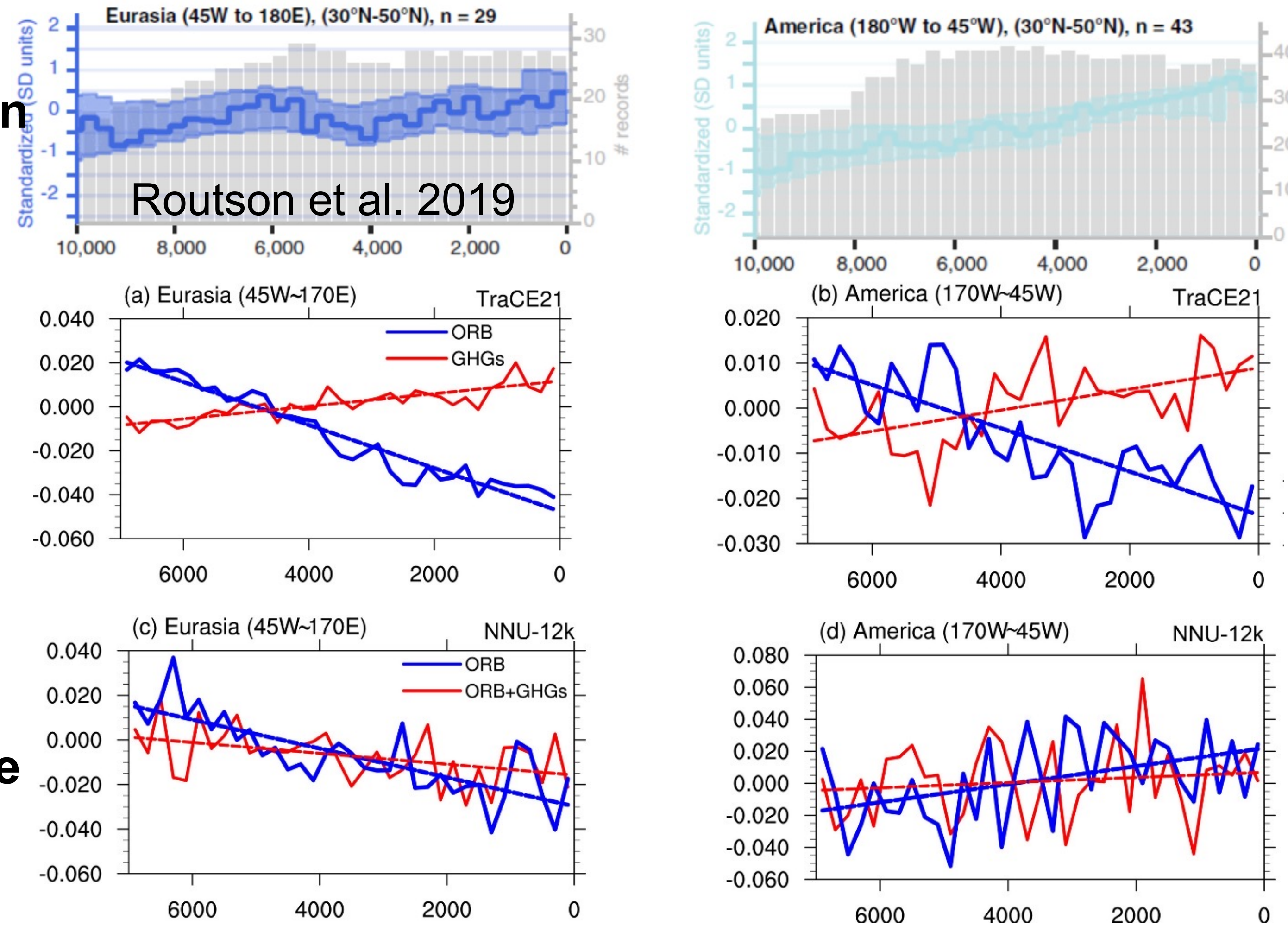

1) Both models simulate **a stronger drying trend over mid-latitude Eurasia** than North America, which is induced by the **ORB**. GHGs contribute to the enhanced precipitation in Eurasia, but it cannot offset the negative contribution of the ORB.
2) The response of simulated NH mid-latitude precipitation to ORB and GHGs is **strongly model dependent**, which is an important factor for the **proxy-model data comparison**.

(Sun et al. 2020, *Quaternary Sciences*)

Result 1: Millennial scale climate responses to external forcings in NNU-Holocene

2. Northern Hemisphere land monsoon precipitation increased by the Green Sahara during mid-Holocene

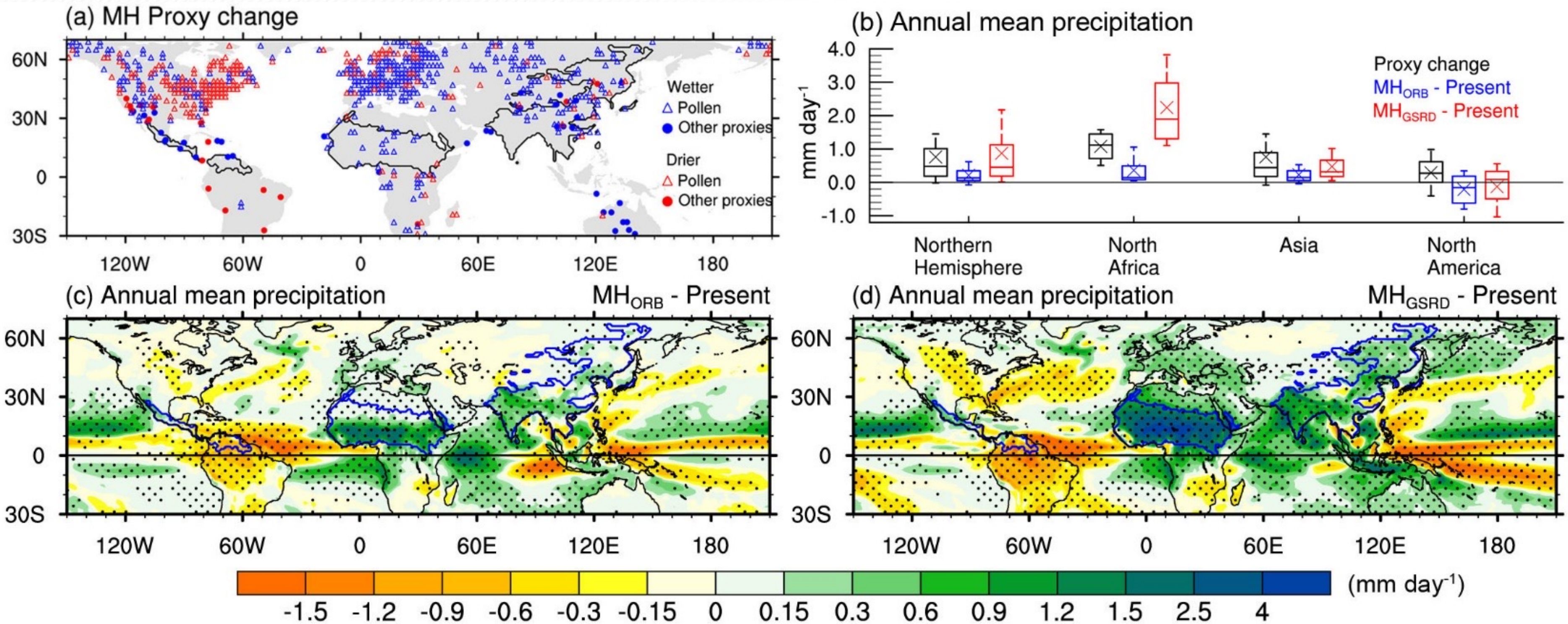

Most of the NHLMP changes revealed by proxy data are reproduced by the model results when the Saharan vegetation cover and dust reduction are taken into consideration. The simulated NHLMP significantly increases by 33.10% under the effect of the Green Sahara, through the large-scale atmospheric circulation changes.

(Sun et al., 2019. *Geophys. Res. Lett.*)

Result 1: Millennial scale climate responses to external forcings in NNU-Holocene

3. Middle East climate response to the Saharan vegetation collapse during the mid-Holocene

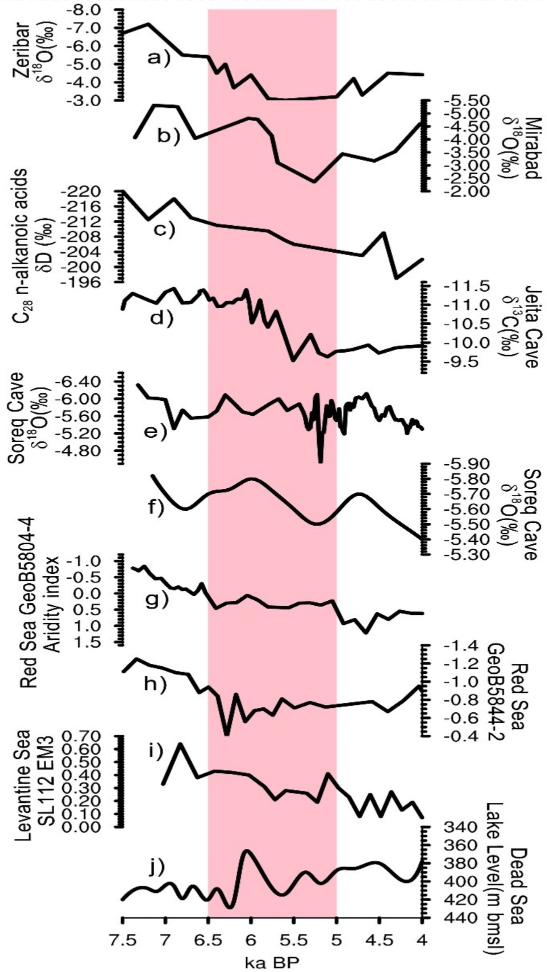

Proxies suggested a drying trend during 6.5 - 5.0 ka and a 5.2 ka drought event.

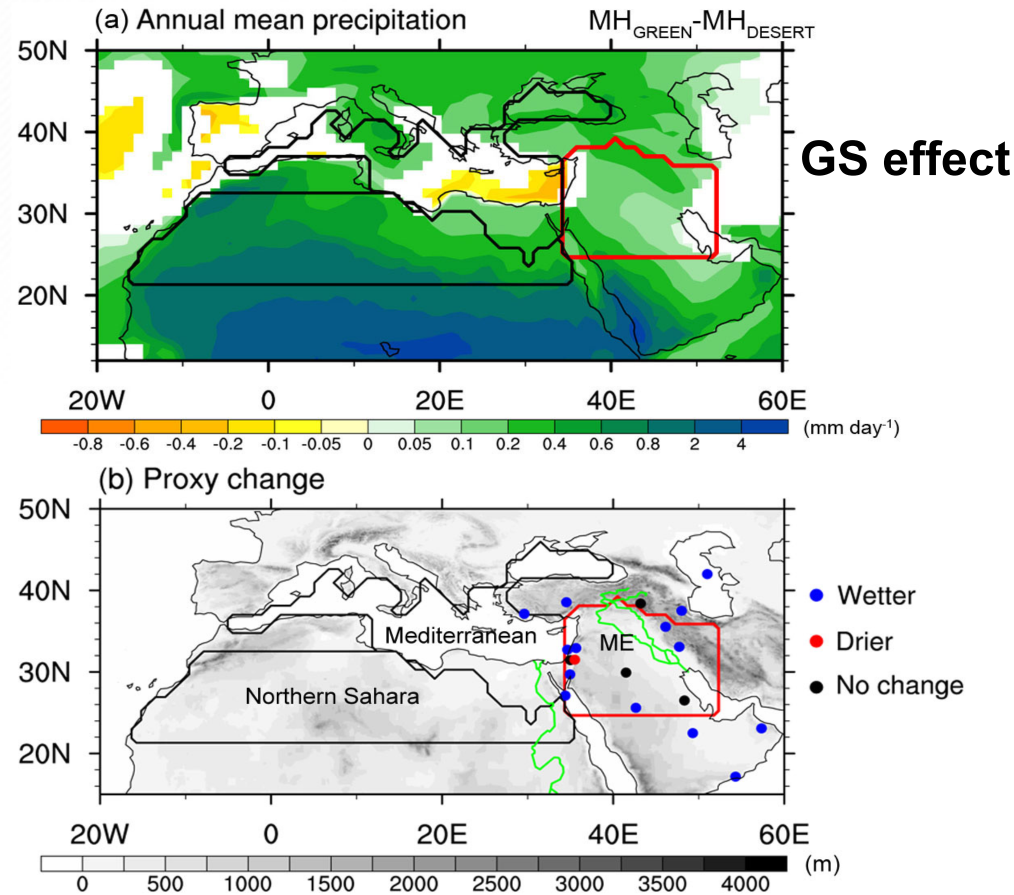

MHgreen minus MHorb experiments suggests a wet ME, which means that the **ME drying trend** can be affected by the **Saharan vegetation collapse**.

(Sun et al. 2020, *J. Climate*)

Result 1: Millennial scale climate responses to external forcings in NNU-Holocene

ME Precipitation enhanced during **FMA**, which **does NOT result from** the enhanced North African monsoon (a) or Mediterranean climate (b).

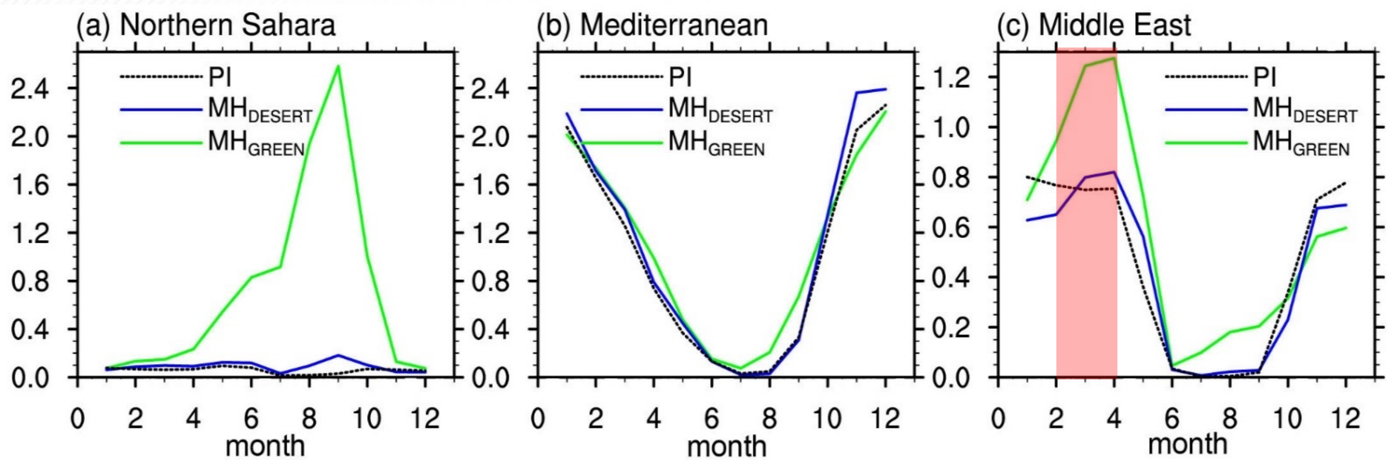

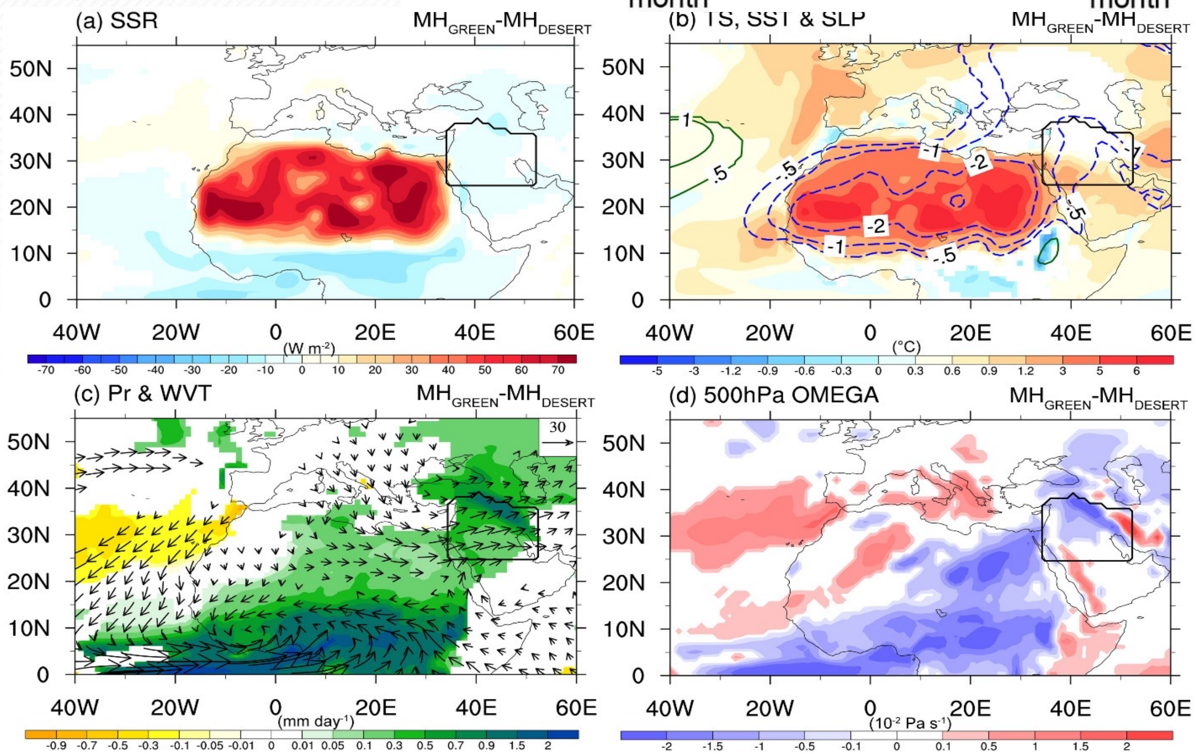

Green Sahara enhances North African warming, inducing the moisture transport from the Red Sea and Mediterranean to the ME.

(Sun et al. 2020, *J. Climate*)

Result 2: Mechanisms behind the 4.2 ka BP event

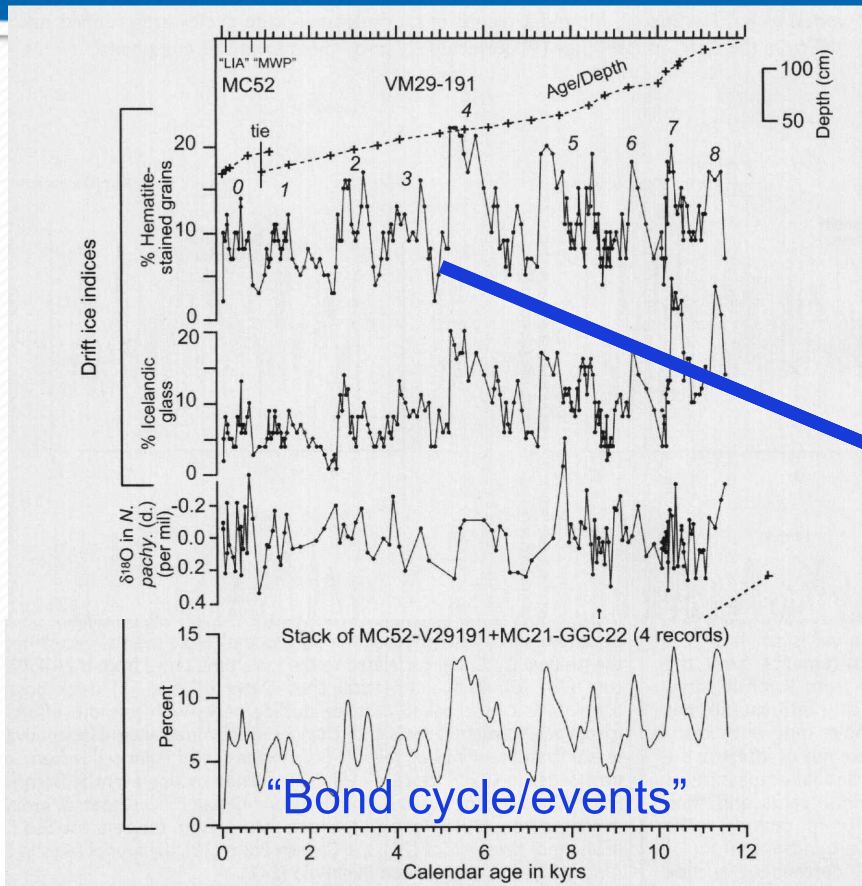

(Bond et al., 2001, *Science*)

One of the Bond events in the Holocene, the 4.2-3.9 ka BP megadrought resulted in synchronous collapse of the Akkadian Empire in Mesopotamia, the Old Kingdom in Egypt and Early bronze Age settlements in Anatolia, the Aegean and the Levant.

(Weiss, 2016, *PAGES*)

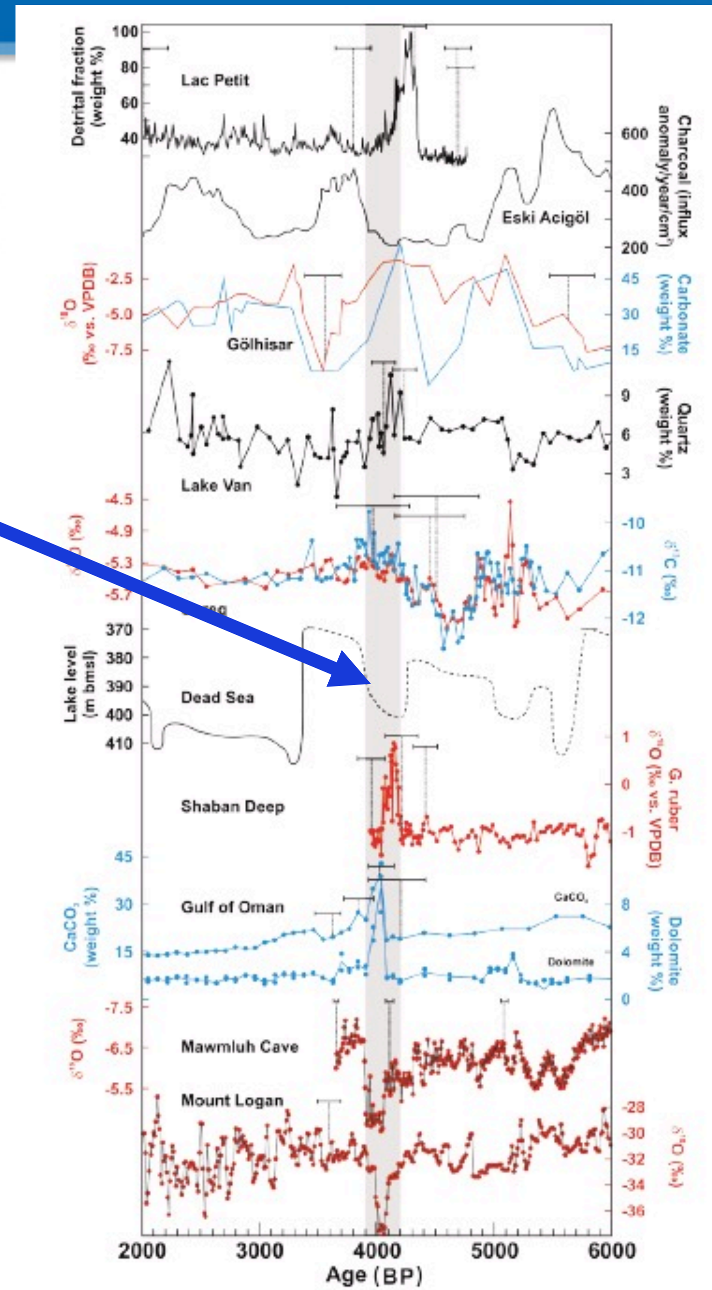

Result 2: Mechanisms behind the 4.2 ka BP event

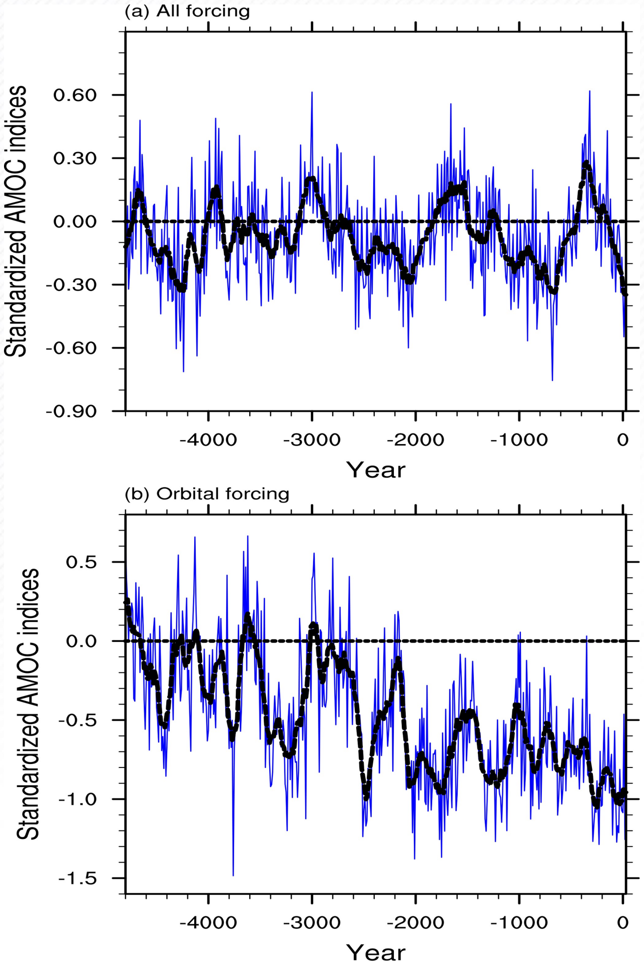

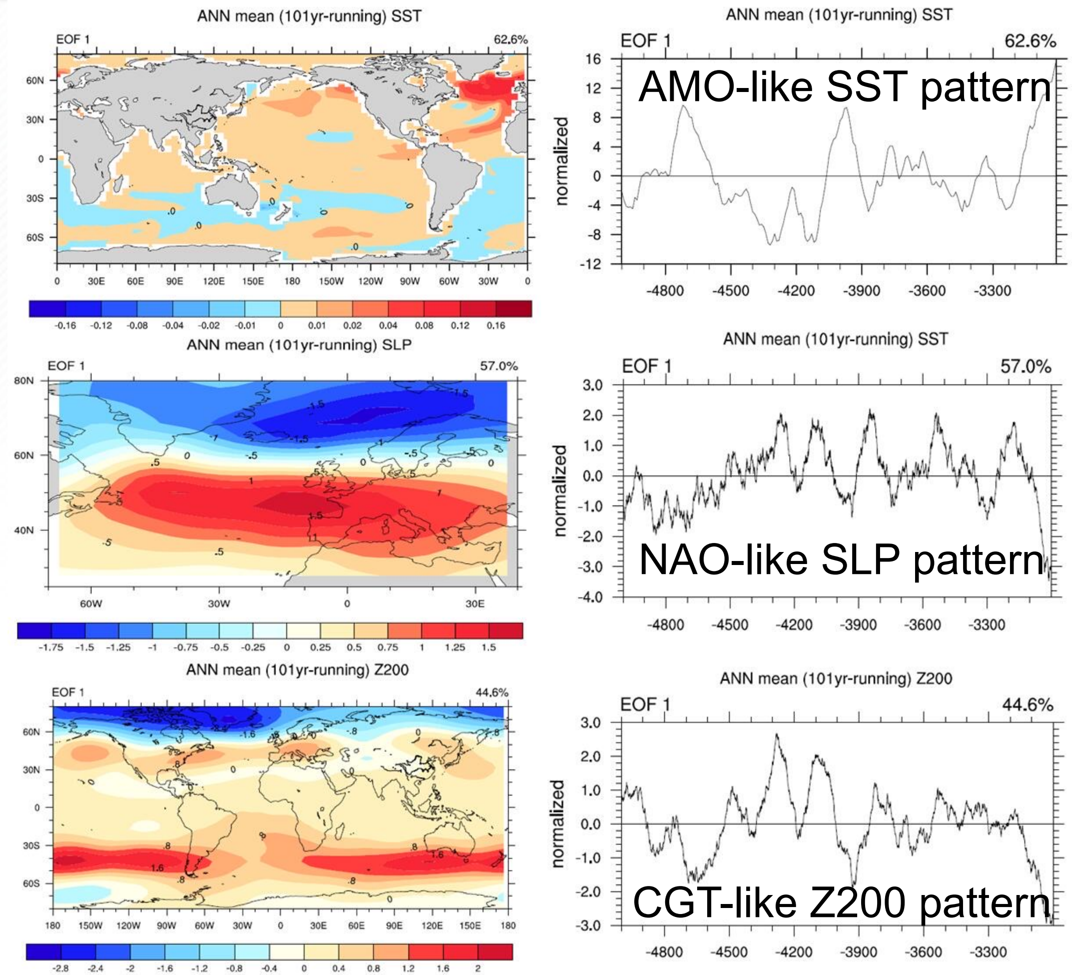

4.2 ka BP event may be induced by multi-century-scale fluctuations in SSTs across the North Atlantic and AMOC strength, superimposed on the steady decline in SSTs and a reduction in the AMOC led by long-term changes of orbital forcing.

(Ning et al., 2019, *Climate of the Past* ; Yan et al., 2019, *Climate of the Past*)

Result 2: Mechanisms behind the 4.2 ka BP event

Comparison between 4.2 ka BP event and 8.2 ka BP event

4.2 ka BP event

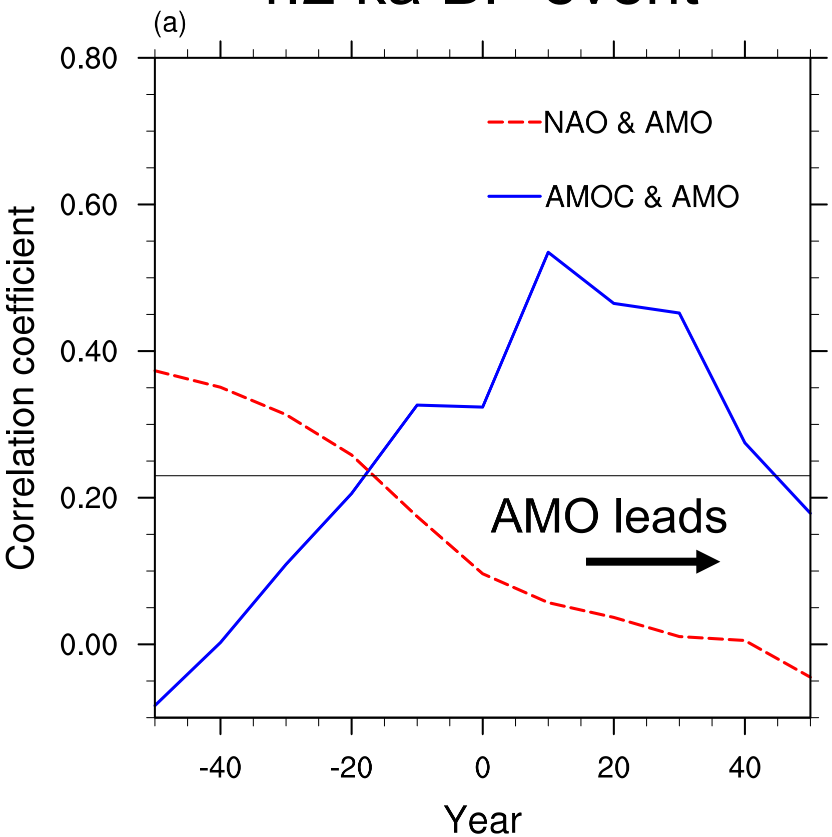

NAO → AMO → AMOC

8.2 ka BP event

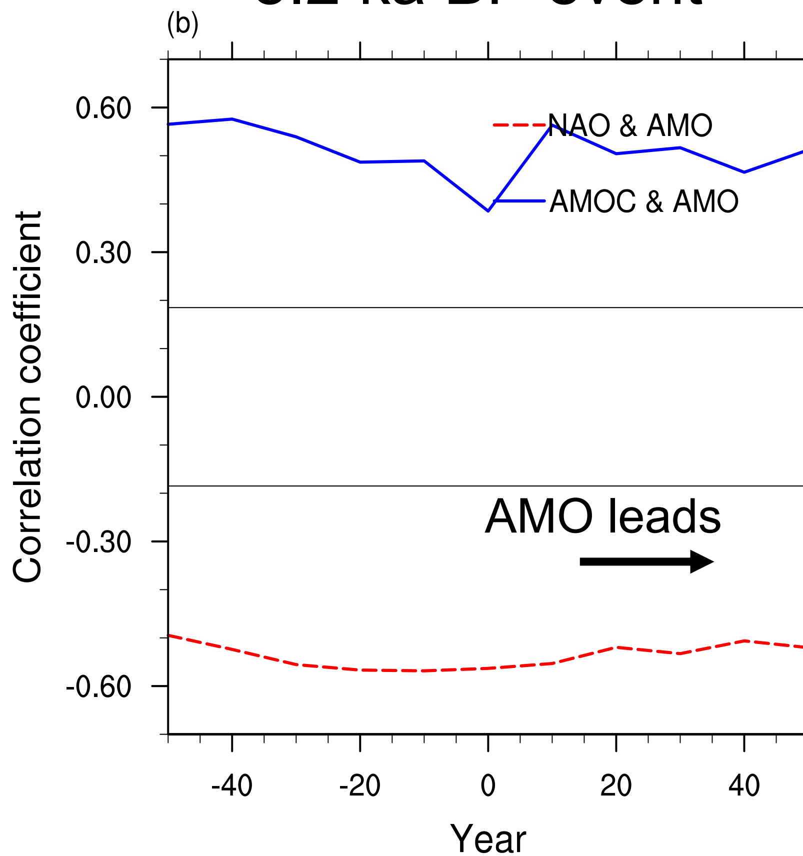

AMOC → AMO → NAO

(Ning et al., 2019, *Climate of the Past* ; Yan et al., 2019, *Climate of the Past*)

Result 3: Mechanisms of decadal megadroughts over eastern China

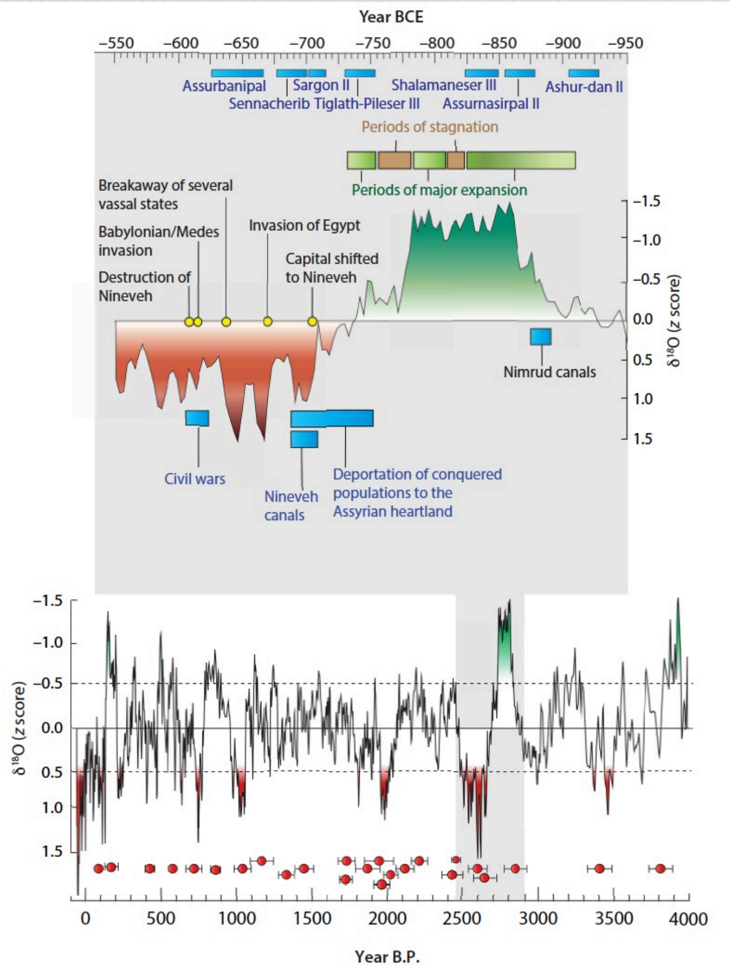

Decadal megadrought during the early mid-seventh century BCE contributed to the eventual political and economic collapse of Assyria.

(Sinha et al., 2019, *Sci. Adv.*)

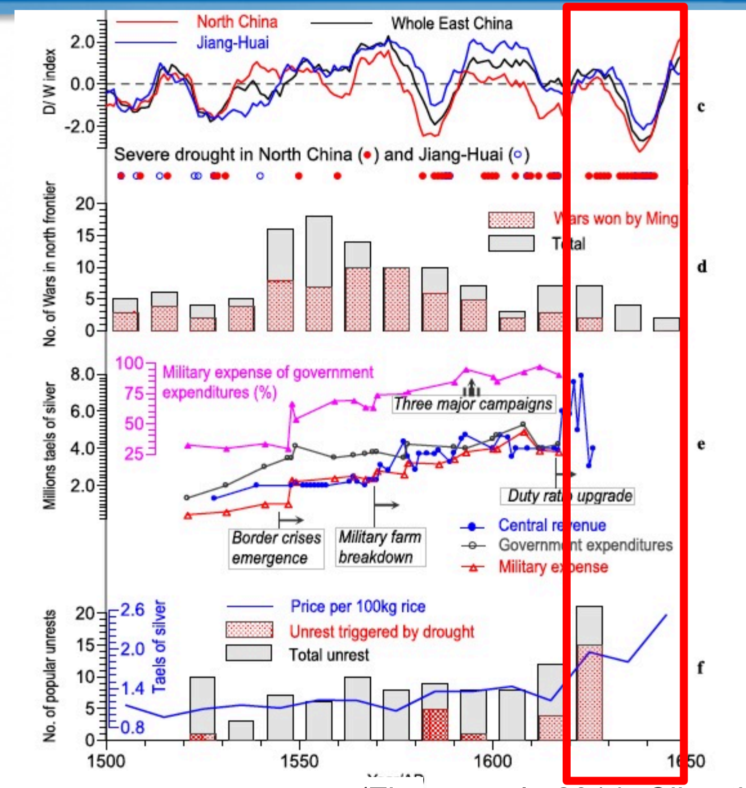

(Zheng et al., 2014, *Climatic Change*)

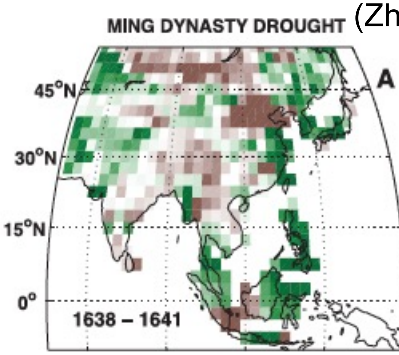

(Cook et al., 2010, *Science*)

Ming Dynasty Megadrought around 1640 contributed to the collapse of Ming Dynasty.

Result 3: Mechanisms of decadal megadroughts over eastern China

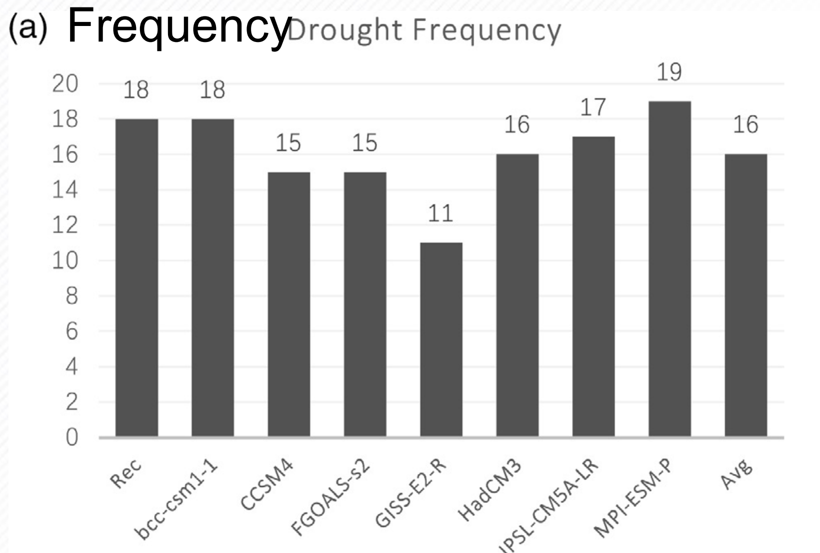

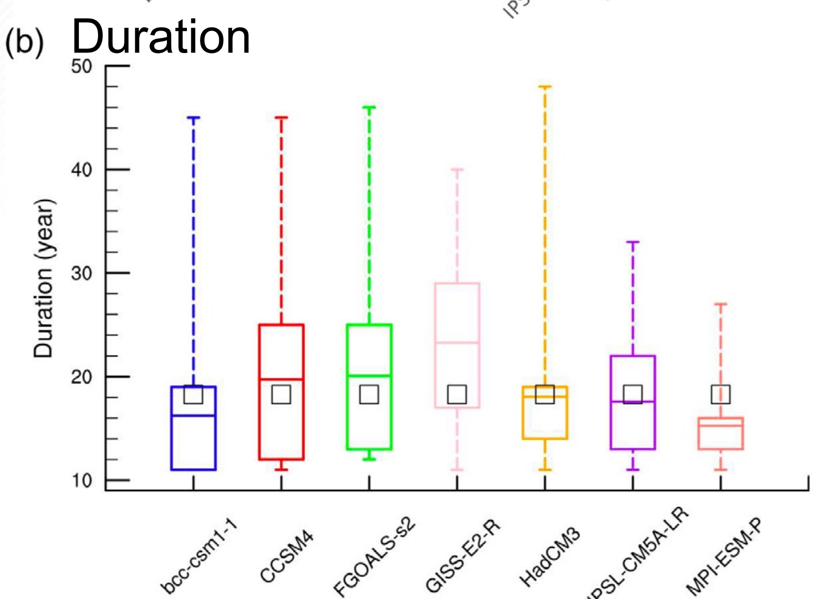

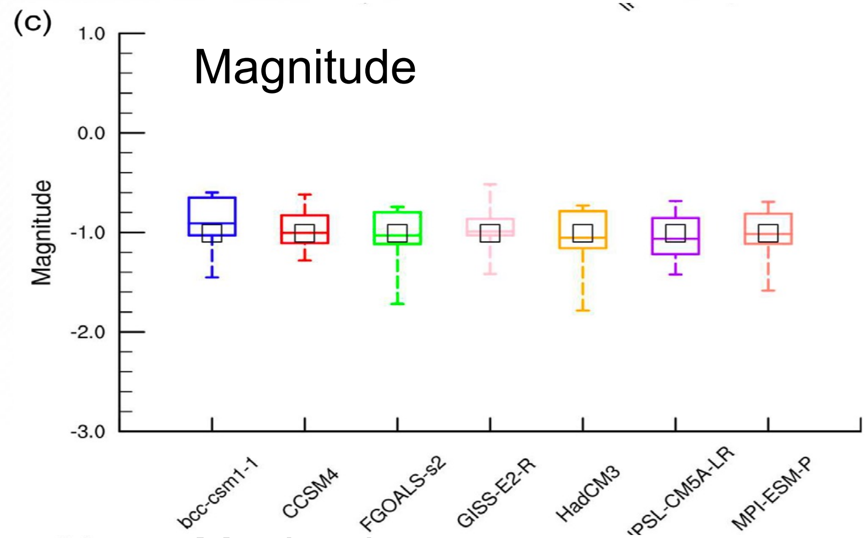

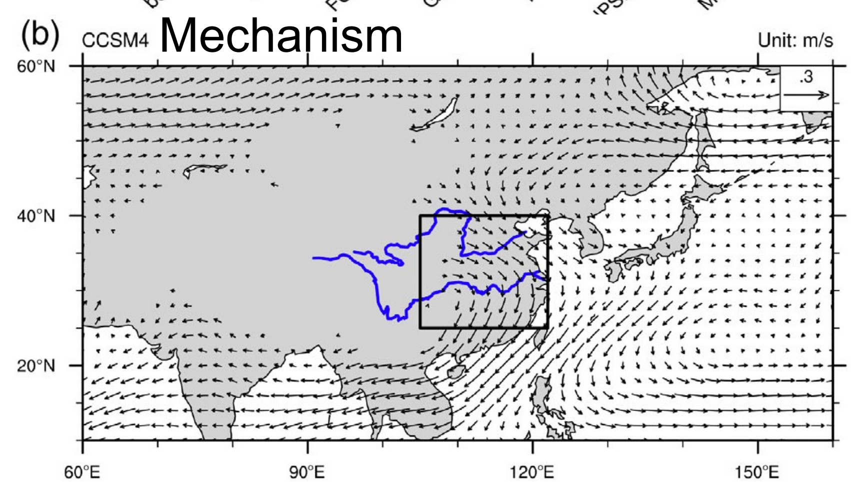

Compared with reconstruction, the simulated megadroughts have similar frequencies, durations, magnitudes, and also the mechanism of weaker EASM.

(Qin et al., 2020, *Int. J. Climatology;* Ning et al., 2019, *Atmos.*)

Result 3: Mechanisms of decadal megadroughts over eastern China

Influences of volcanic eruptions on megadrought frequency

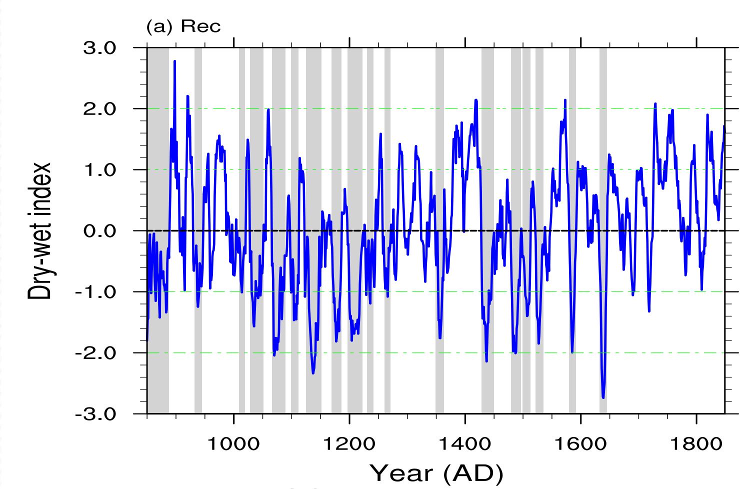

Rec: 18 megadroughts

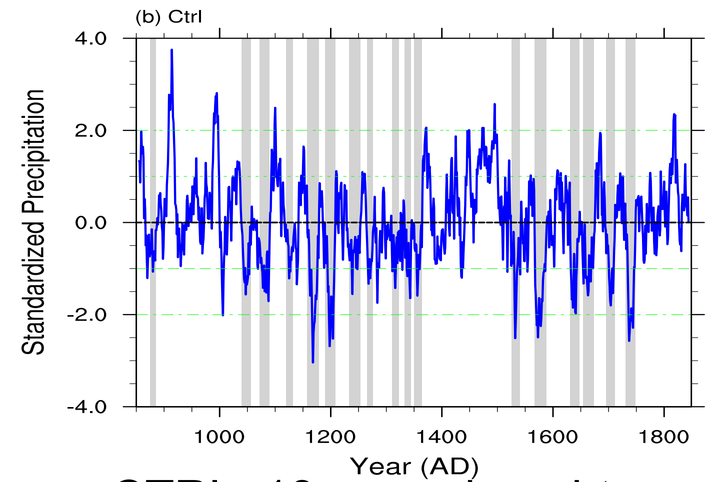

CTRL: 18 megadroughts

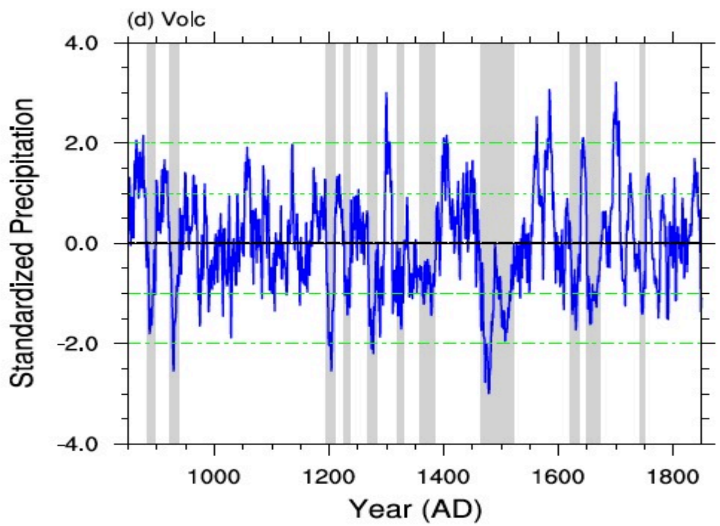

VOLC: 12 megadroughts

	Frequency	Frequency based on PDSI
Reconstruction	18	9 (1360-1850)
CTRL	18	14
VOLC_1	12	14
VOLC_2	17	13
VOLC_3	17	11
VOLC_4	12	12
VOLC_5	12	12
Average of VOLC (standard deviation)	14 (2.74)	12.4 (1.14)

(Ning et al., 2020, *J. Climate*)

Result 3: Mechanisms of decadal megadroughts over eastern China

Mechanisms behind the influences

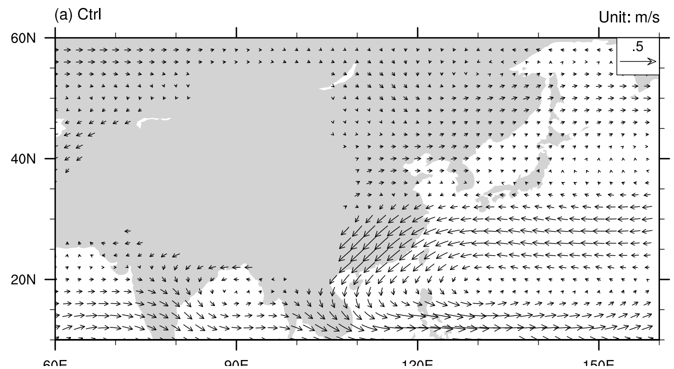

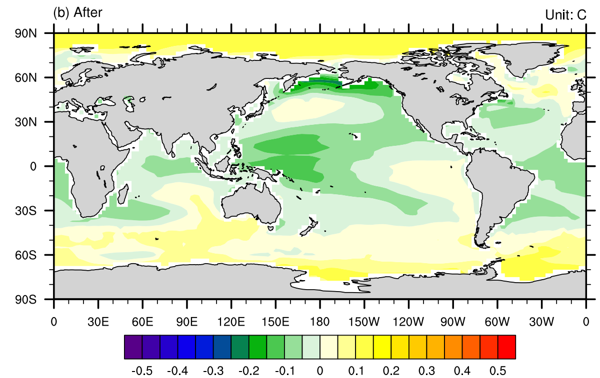

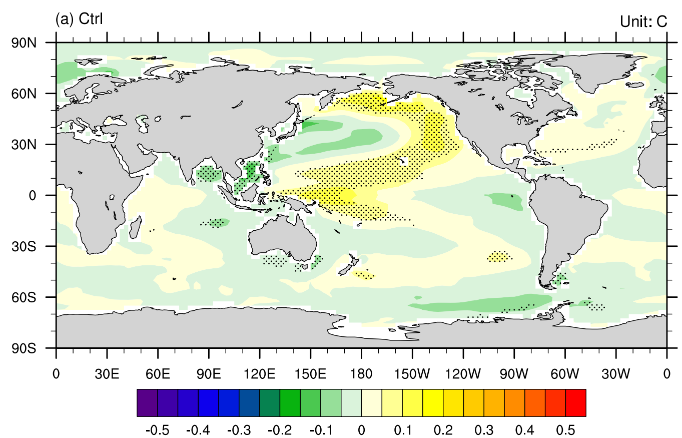

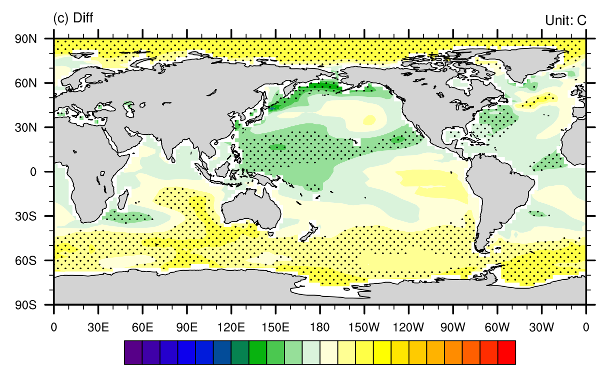

After removing the direct influence of volcanic eruptions, the SST anomalies over the Pacific resemble a negative PDO-like pattern.

Decadal megadroughts over the eastern China are associated to weaker EASM, corresponding to a positive PDO-like SSTA pattern.

(Ning et al., 2020, *J. Climate*)

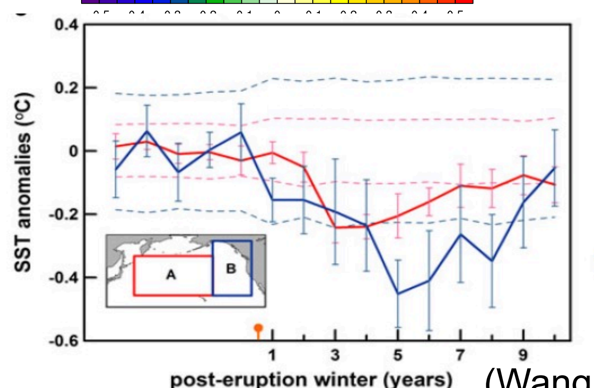

(Wang et al., 2012)

Result 3: Mechanisms of decadal megadroughts over eastern China

Case study: Ming Dynasty Drought

- The Ming Dynasty Drought that lasts for period 1637-1643 with largest precipitation decrease around 1640, appears to be the severest drought over China during last five centuries, and may have contributed to the fall of the Ming Dynasty at 1644 (Zheng et al., 2006; Cook et al., 2010).

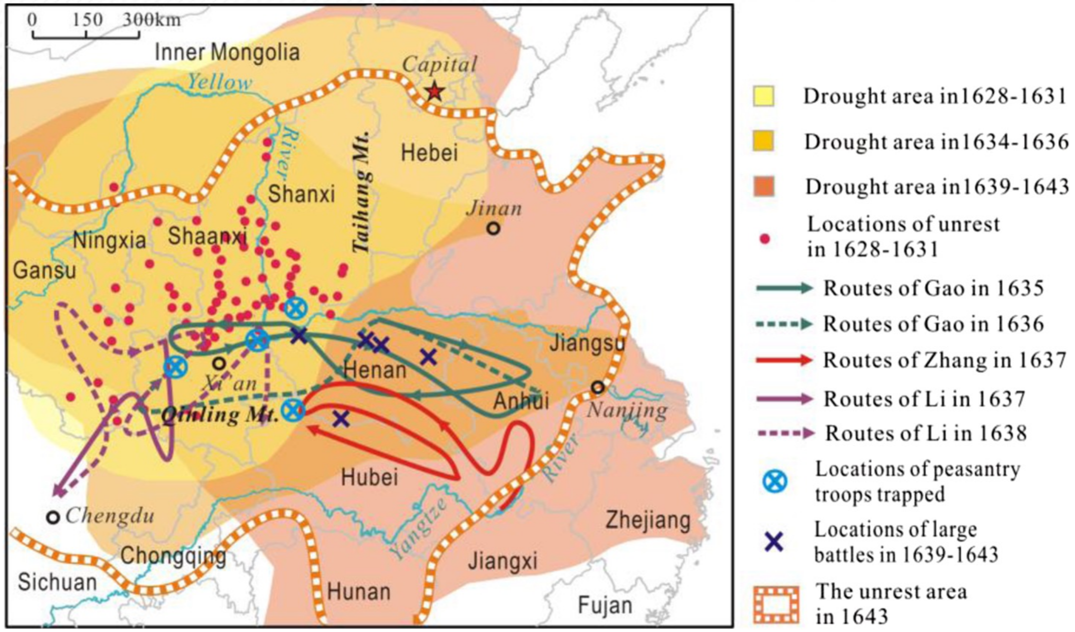

(Zheng et al., 2014)

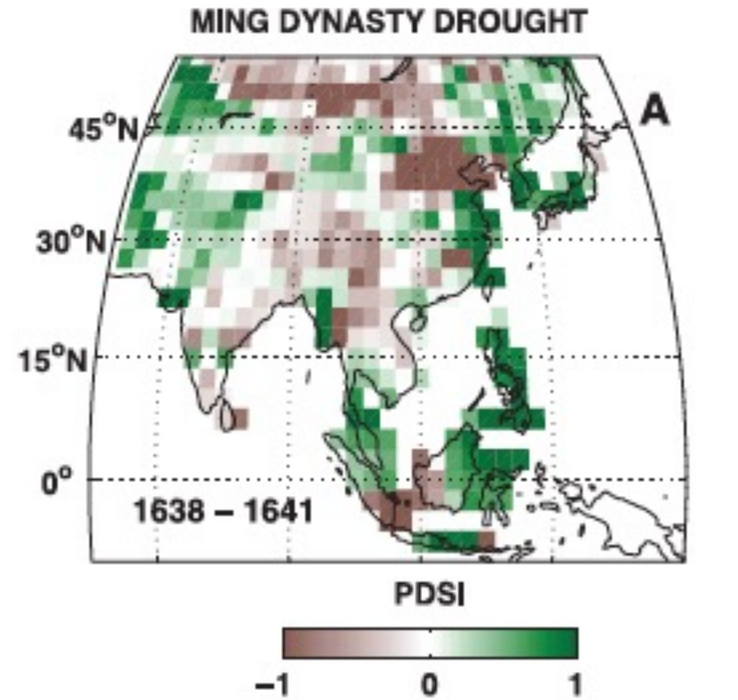

(Cook et al., 2010)

Result 3: Mechanisms of decadal megadroughts over eastern China

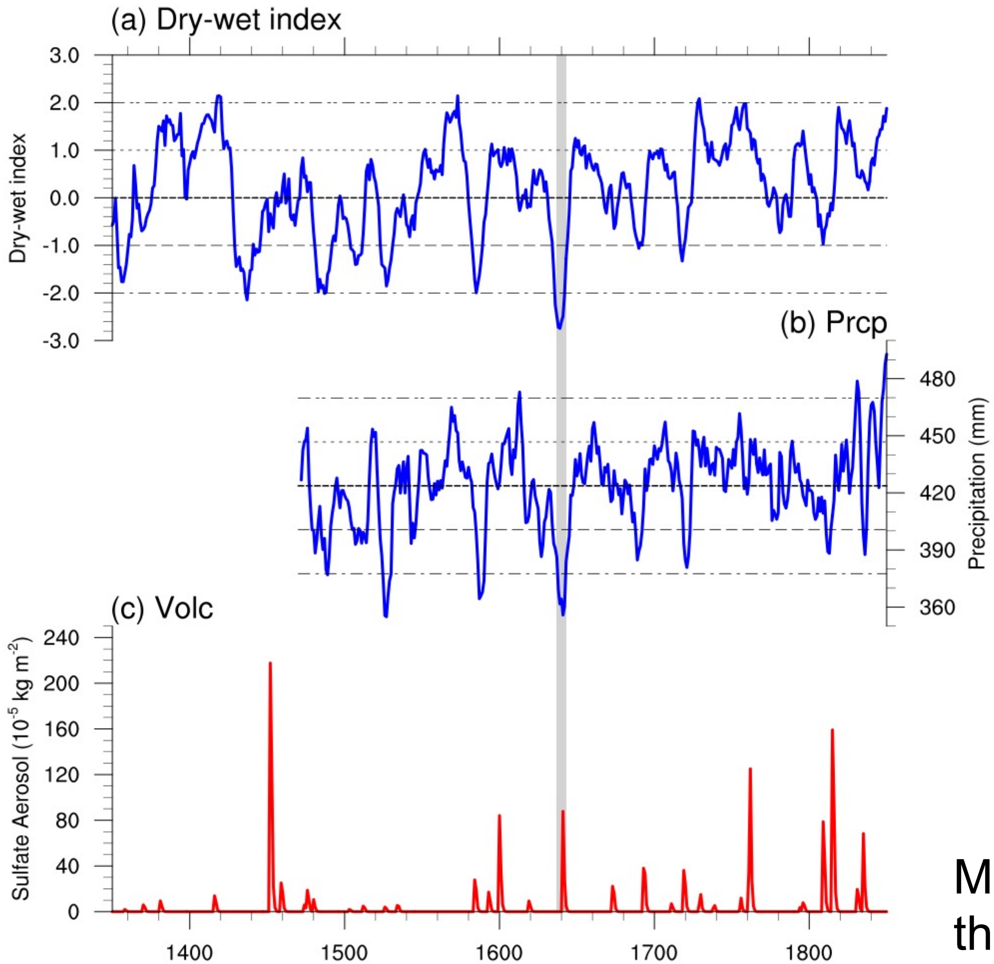

(Chen et al., 2020, *GRL*)

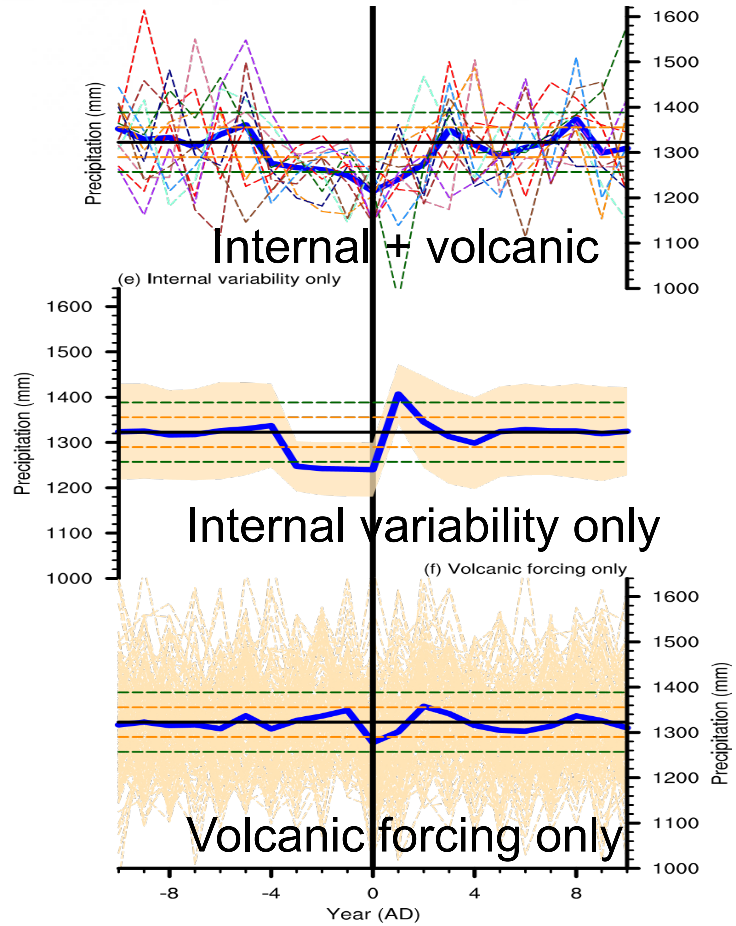

Ming Dynasty Drought is coincident with the volcanic eruption at 1641 at Mt. Parker (Gao et al., 2008; Sigl et al., 2013), but only volcanic eruption cannot trigger a megadrought.

Result 3: … eastern China

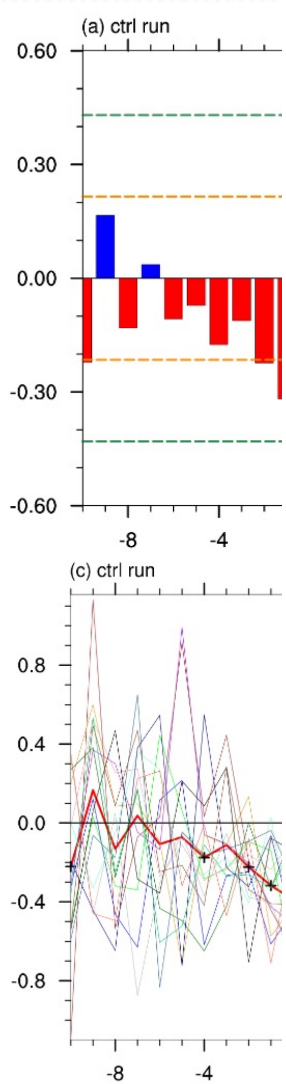

nature

View all Nature Research journals Search Login

Explore our content Journal information Subscribe

nature > research highlights > article

CLIMATE SCIENCES · 25 AUGUST 2020

The eruption that helped to destroy one of China's great dynasties

Cooling particles in a volcanic plume intensified the drought that toppled the Ming dynasty.

***Nature* Research hightlights**

The collapse of China's prosperous Ming dynasty, one of the most stable in Chinese history, has been attributed, in part, to the 1641 eruption of a volcano thousands of kilometres from the imperial capital in Beijing.

Geoscientists have long known that a mega-drought that parched eastern China between 1637 and 1643 was the most severe to affect the area during the last millennium, but they did not know precisely what made it so bad. Liang Ning at Nanjing Normal University in China, Zhengyu Liu at Ohio State University in Columbus and their colleagues looked at records of past temperatures, as well as ice-core records and climate models, to unravel the mystery.

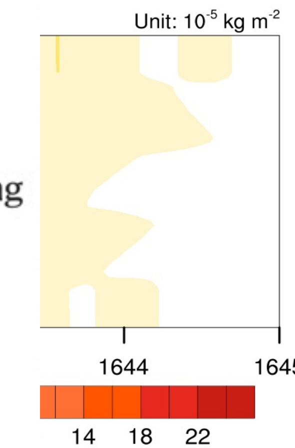

orcing from
ic eruption
hts caused
ability, the
more years
agnitudes,
history.

(Chen et al., 2020, *GRL*)

Result 3: Mechanisms of decadal megadroughts over eastern China

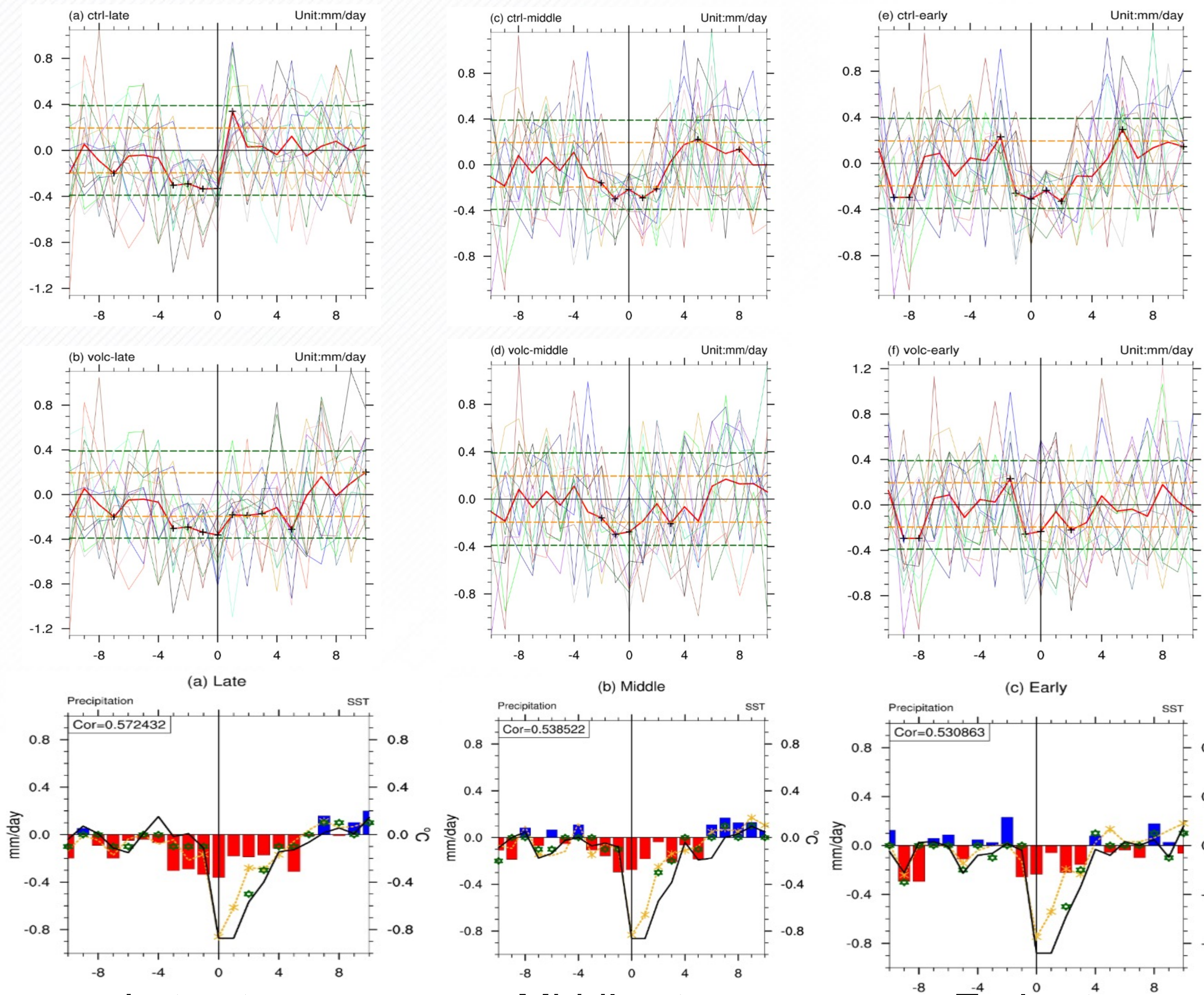

Late stage

Middle stage

Early stage

Volcanic eruptions implement severer influences during the late stage of droughts induced by internal variability, probably due to the soil moisture.

(Chen, et al., 2021, to be submitted)

Result 4: Centennial to decadal climate responses to LUCC

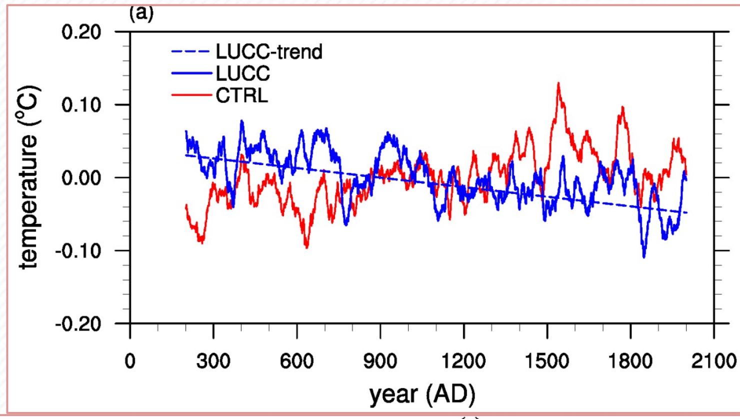

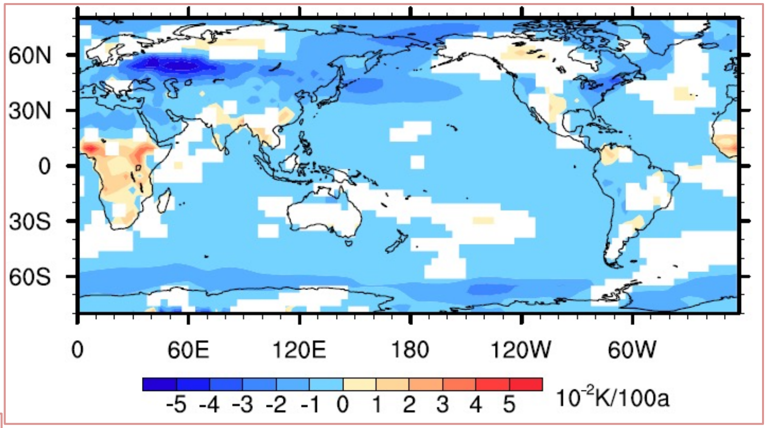

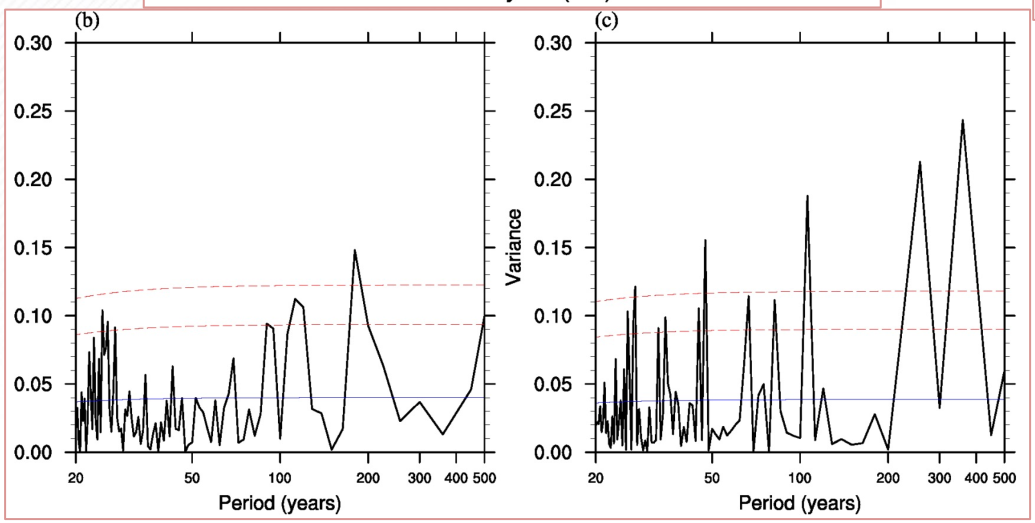

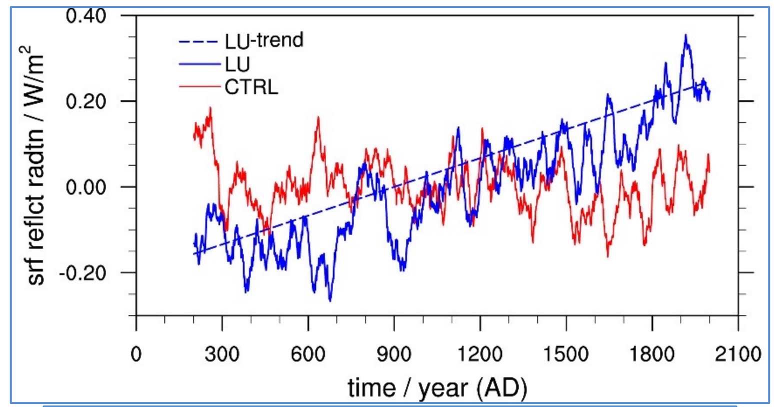

The decreasing trend of temperature is mainly due to the increasing trend of surface reflected solar radiation

From (b) and (c), in the LU sensitivity experiment, the approximate 50-year, 100-year, 300-year and 400-year periods all exceeded the 95% confidence level, which are absent in CTRL run.

(Yan et al, 2017, *Atmos.*)

Result 4: Centennial to decadal climate responses to LUCC

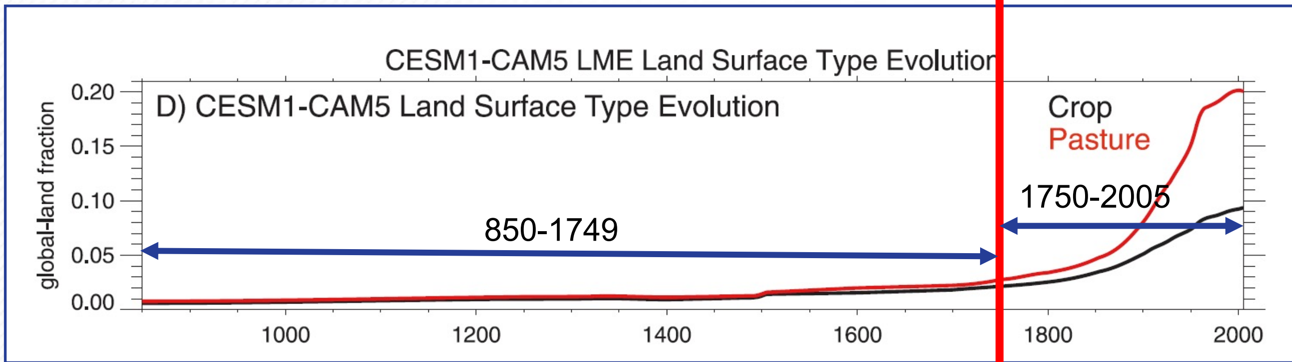

The LUCC forcing used in CESM-LME
(Otto-Bliesner B L, Brady E C, Fasullo J, et al. 2016)

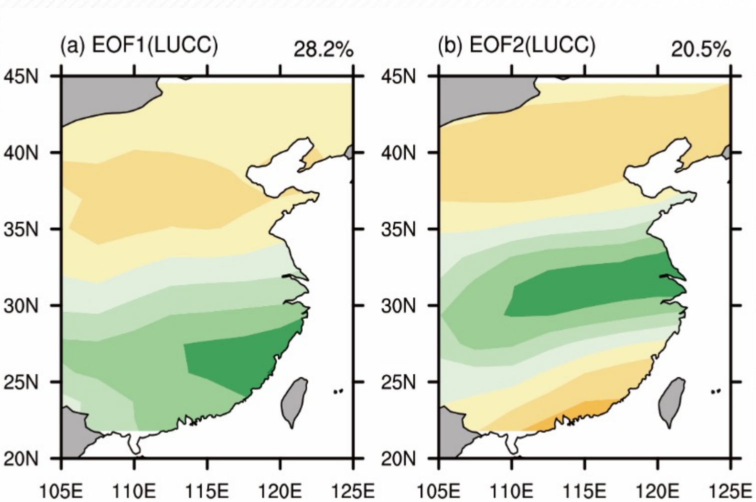

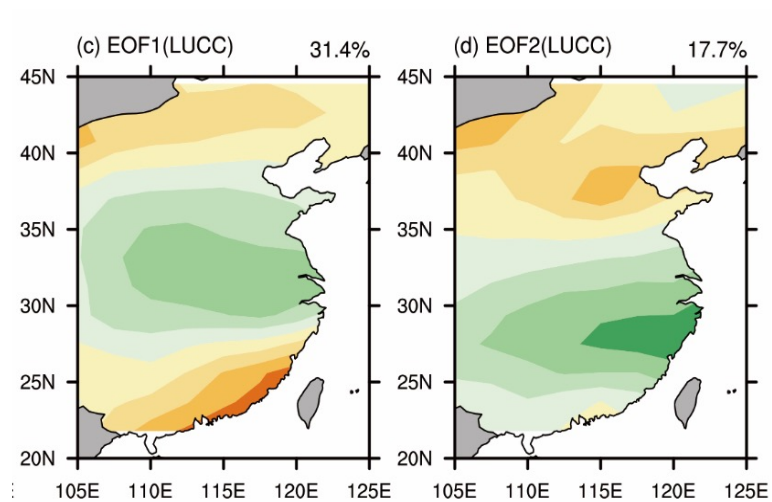

Before 1750

After 1750-2005

(Wang et al., 2020, *Int. J. Climatology*)

Result 4: Centennial to decadal climate responses to LUCC

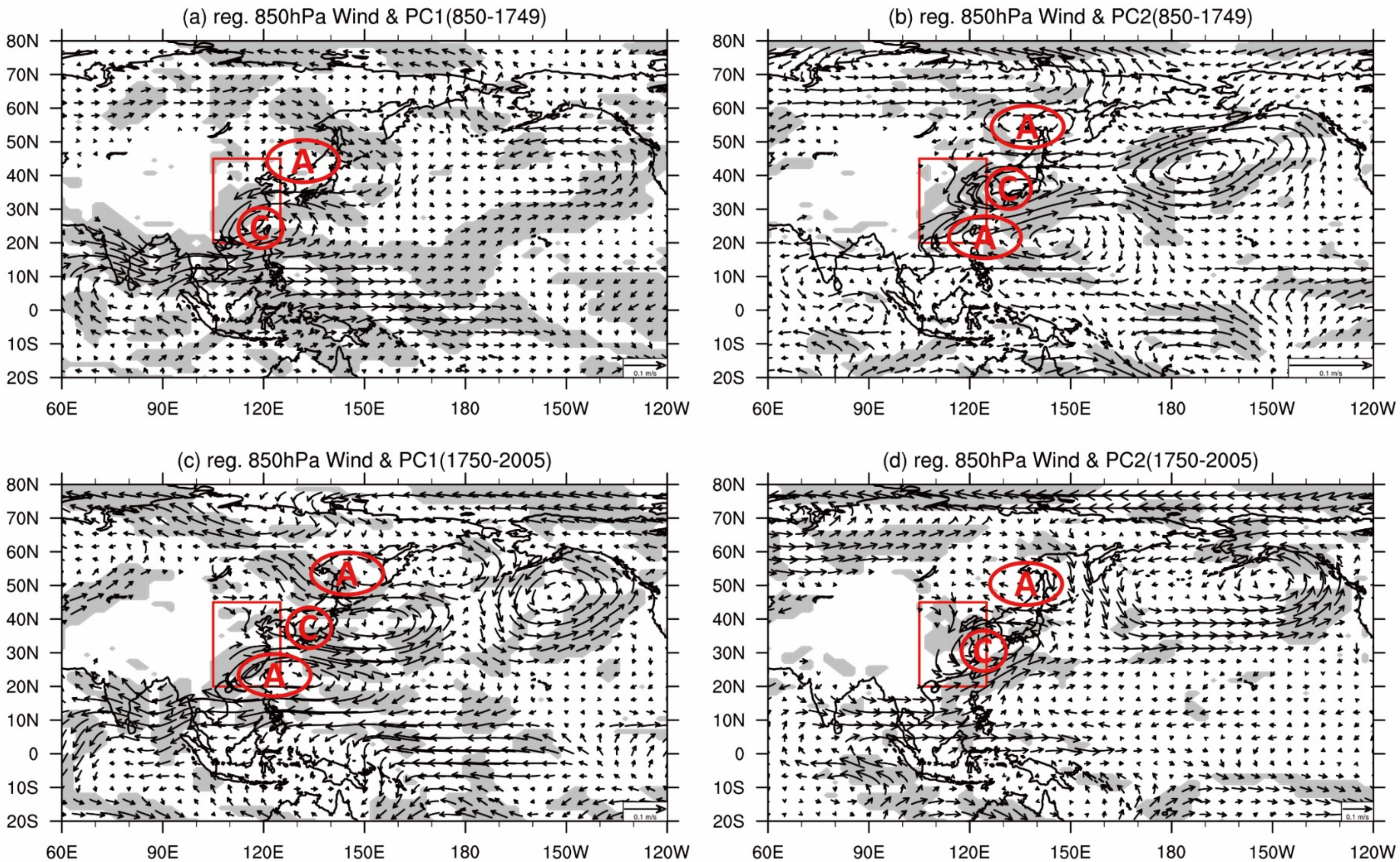

Regressions of 850 hPa winds (unit: m/s) against the PCs of the EOF modes shown in Figure: (a), (b) are the regressions against the PCs before LUCC, and (c), (d) are the regressions against the PCs after LUCC. Dark shading and vectors indicate anomalies that are statistically significant at the 0.05 level.

(Wang et al., 2020, *Int. J. Climatology*)

Result 4: Centennial to decadal climate responses to LUCC

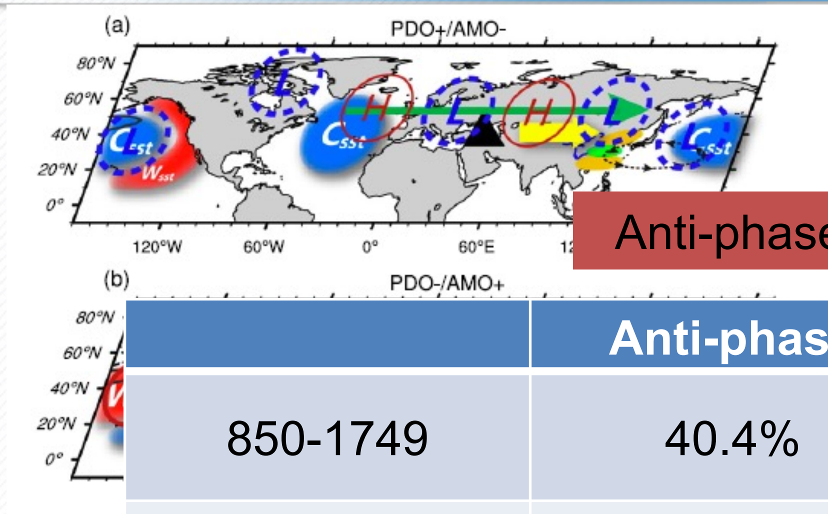

Anti-phase → Tripolar distribution

	Anti-phase	In-Phase
850-1749	40.4%	59%
1749-2005	48%	50%

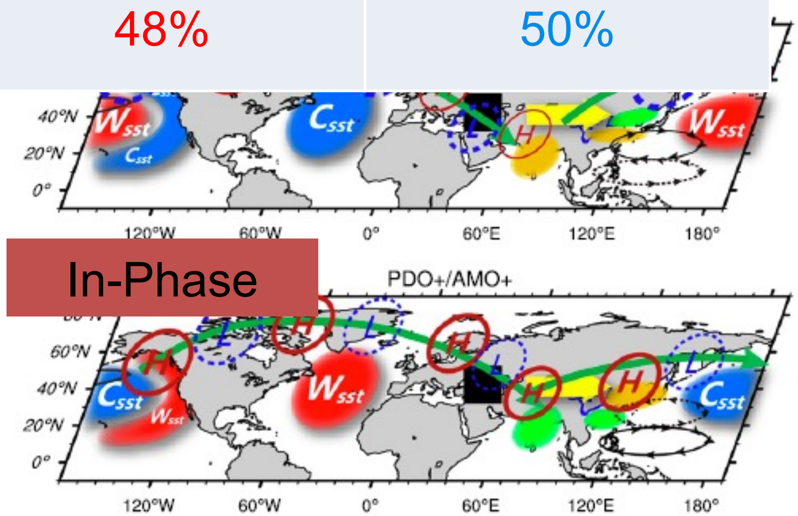

Dipolar distribution ← In-Phase

(Zhang Z et al., 2018)

LUCC induces the increased probability of anti-phases between PDO and AMO, and decreased probability of in-phases between PDO and AMO. Therefore, the occurrences of summer precipitation tripolar distribution over eastern China increase, and the occurrences of dipolar distribution decrease.

(Wang et al., 2020, *Int. J. Climatology*)

Result 5: Influences of TSI on decadal EAM variability

1. A centennial episode of weak EASM in the MCA

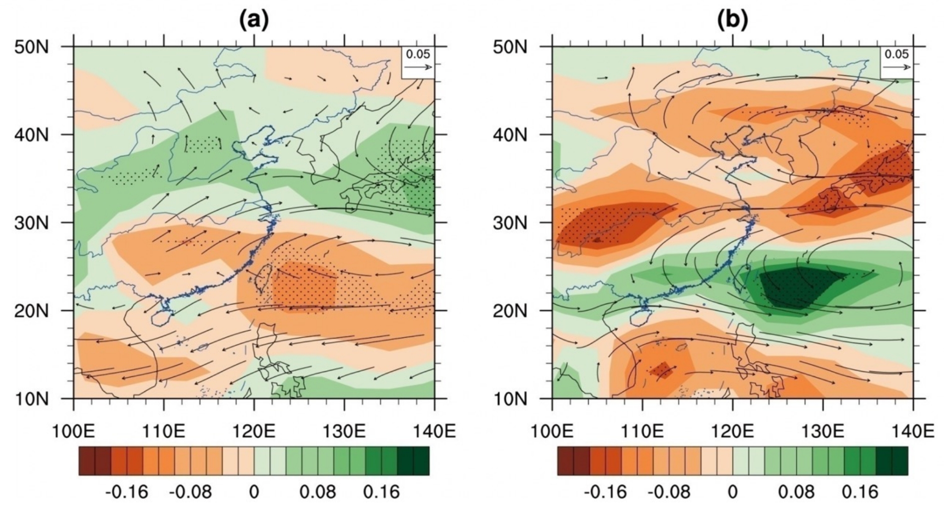

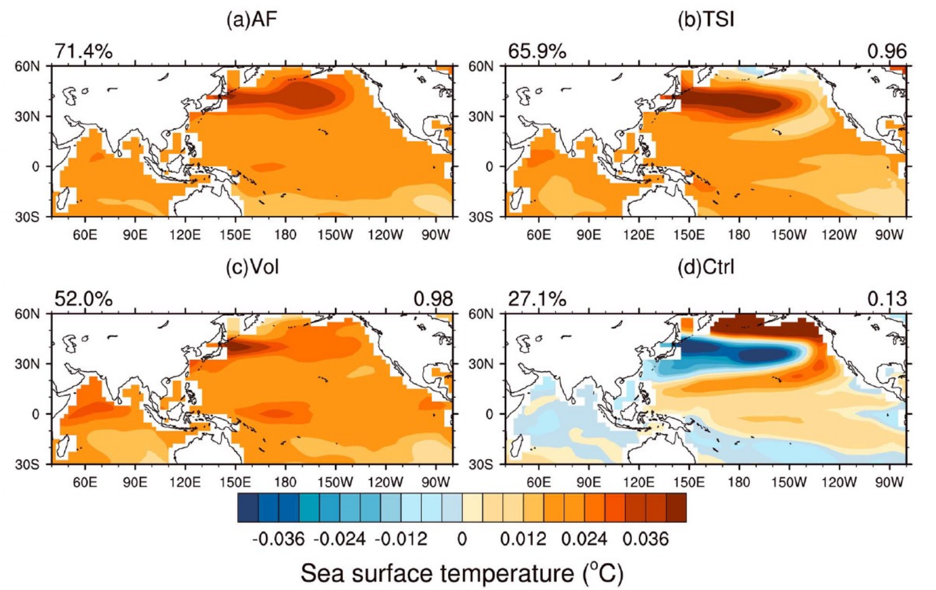

A centennial episode of drought relevant to weak EASM (980-1100) in the MCA (801-1250) was found. This weakening of the EASM during 11th century in the middle of the MWP is mainly attributed to the low solar radiation during that period.

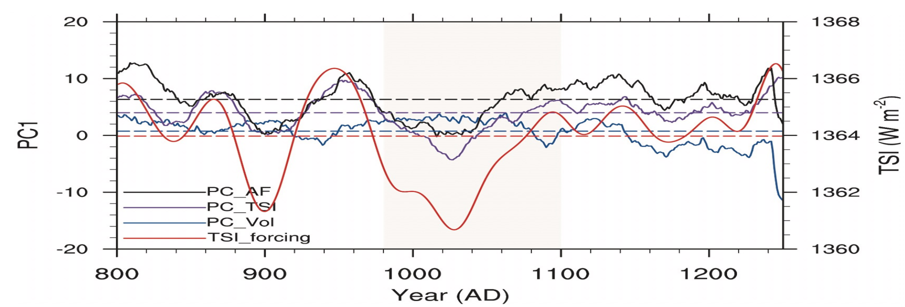

(Jin et al., 2018, *Paleoceanography and Paleoclimatology*)

Result 5: Influences of TSI on decadal EAM variability

2. Decadal variations of the East Asian summer monsoon forced by the 11-year insolation cycle

CESM-LME （SSI experiment）

Strong 11-yr solar cycle epoch (AD 900-1285)
Weak 11-yr solar cycle epoch (AD 1400-1535)

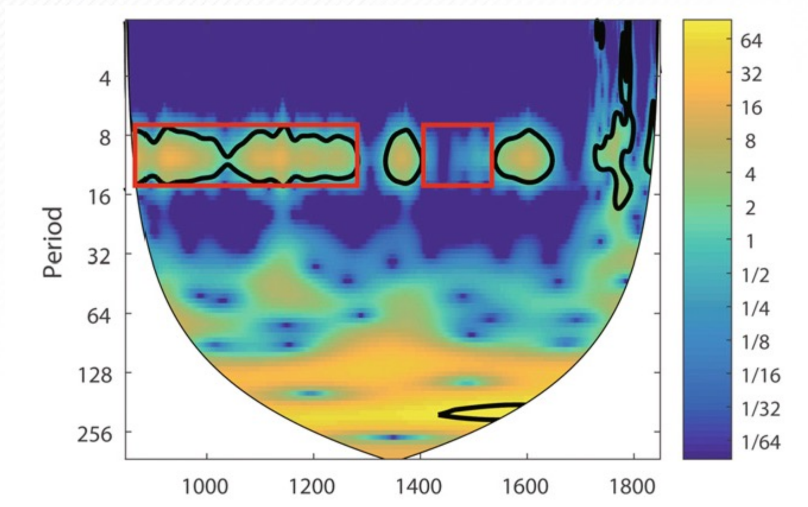

Wavelet analysis of the external forcing used in the solar only forcing experiments.

Strong 11-yr solar cycle epoch **Weak 11-yr solar cycle epoch**

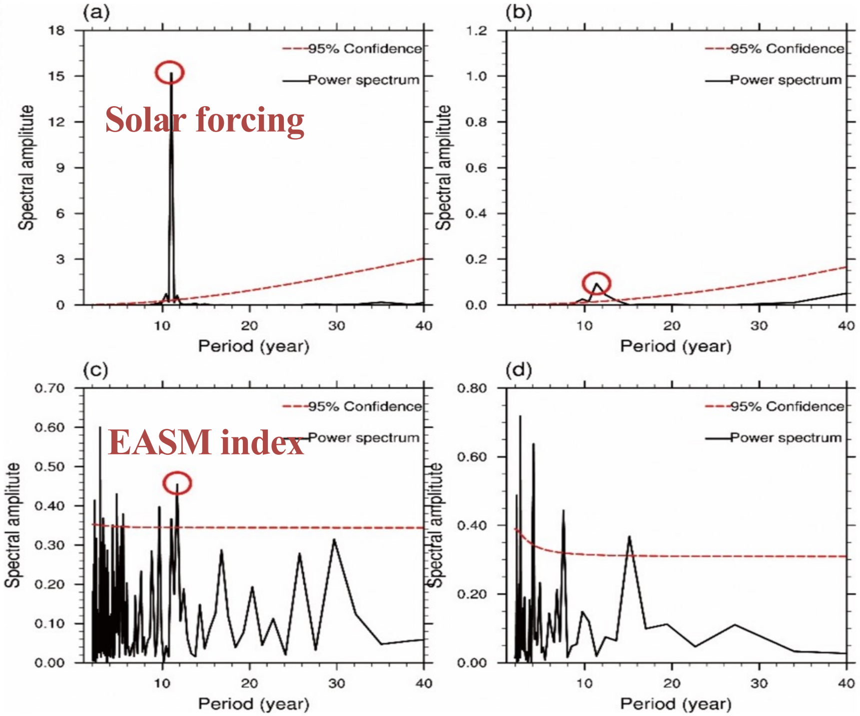

During the AD 900–1285 epoch with strong 11-yr solar cycle **(a)**, the EASM index has a conspicuous peak at approximately 11 years **(c)**, whereas during the insignificant forcing epoch of AD 1400–1535 **(b)**, the quasi-11-yr periodicity disappears **(d)**.

(Jin et al., 2019, *Journal of Climate*)

Result 5: Influences of TSI on decadal EAM variability

2. Decadal variations of the East Asian summer monsoon forced by the 11-year insolation cycle

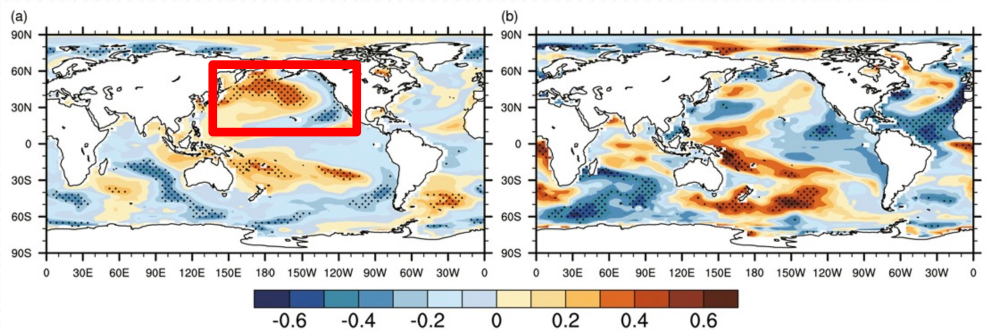

Simultaneous correlation map of the MJJAS mean SST of SSI experiments with **external forcing** on the decadal time scale during the (a) strong 11-yr solar cycle epoch and (b) weak 11-yr solar cycle epoch.

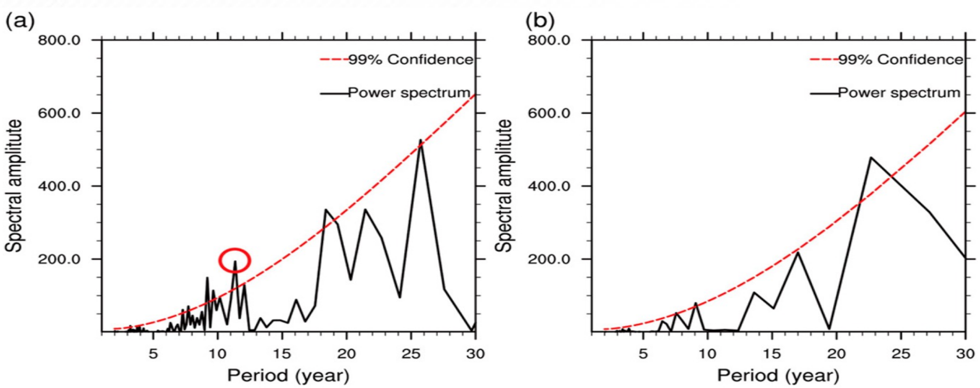

Power spectrum of the **PDO index** of SSI experiments during the (a) strong 11-yr solar cycle epoch and (b) weak 11-yr solar cycle epoch.

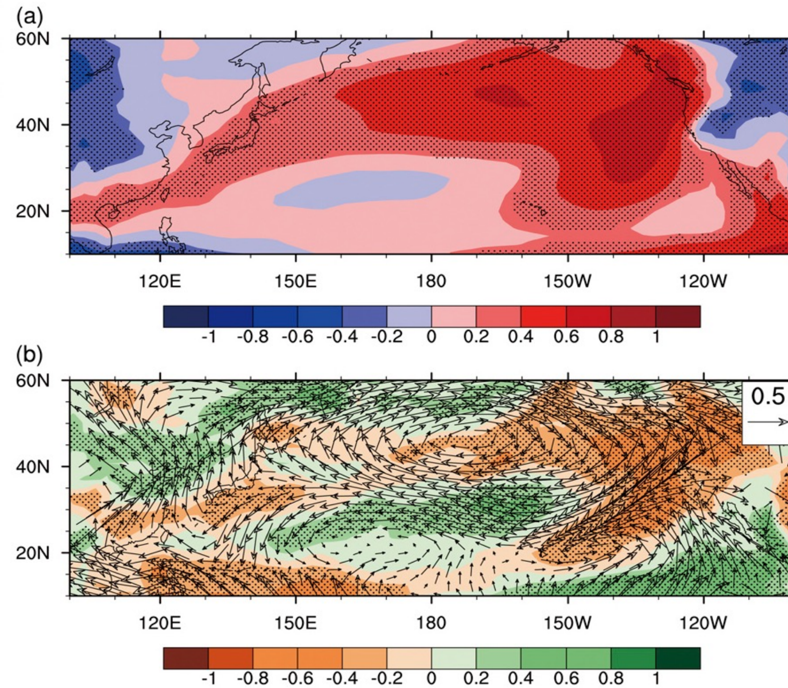

A strong, 11-yr solar cycle excites an anomalous SST pattern that resembles a cool Pacific decadal oscillation (PDO) phase with a significant 11-yr periodicity, which then results in abundant rainfall over northern EA.

(Jin et al., 2019, *Journal of Climate*)

Result 5: Influences of TSI on decadal EAM variability

3. Decadal variability of northern Asian winter monsoon shaped by the 11-year solar cycle

The two leading EOF modes of the DJF mean surface temperature over Asia

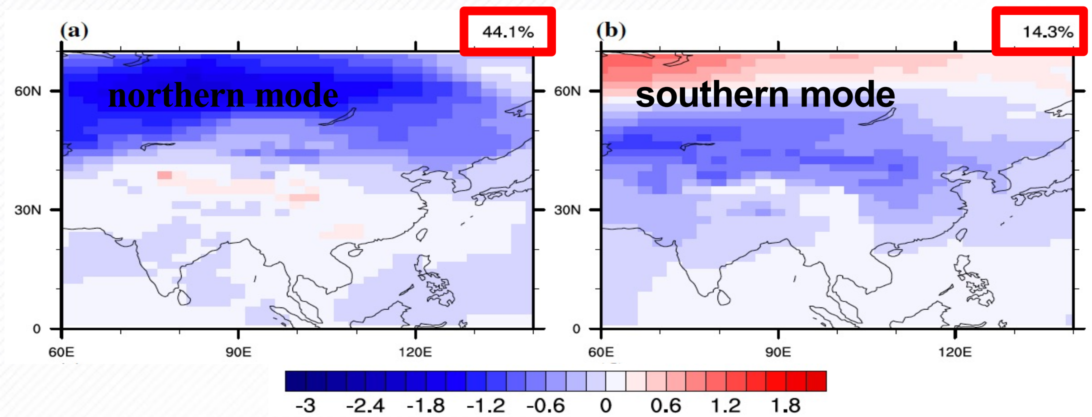

Only the EOF1 has been discussed due to the higher explanation of the total variance.

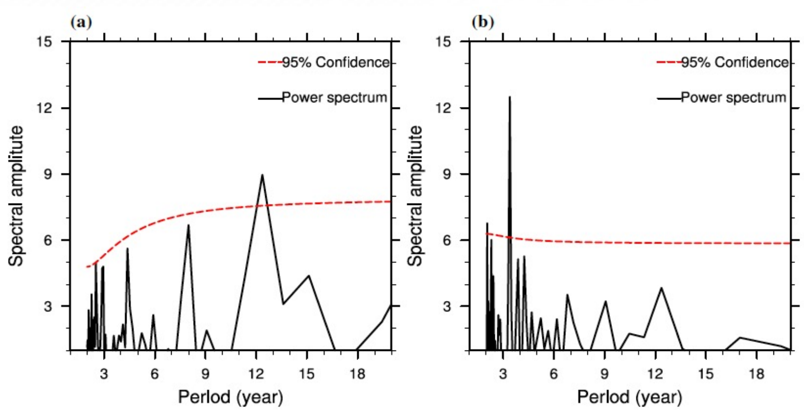

A significant decadal signal exists in the PC1 during the strong epoch, but absent during the weak epoch.

The **leading mode** of the AWM reaches the strongest phase **4 years after the maximum solar irradiance (a)**, but is approximately **in phase with the accumulated total solar irradiance (b)**.

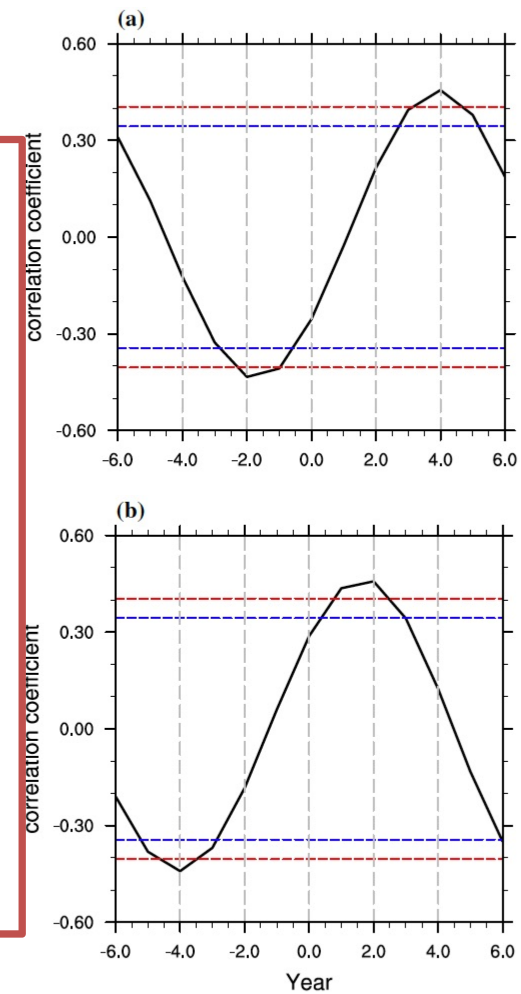

(Jin et al., 2019, *Climate Dynamics*)

Result 5: Influences of TSI on decadal EAM variability

3. Decadal variability of northern Asian winter monsoon shaped by the 11-year solar cycle

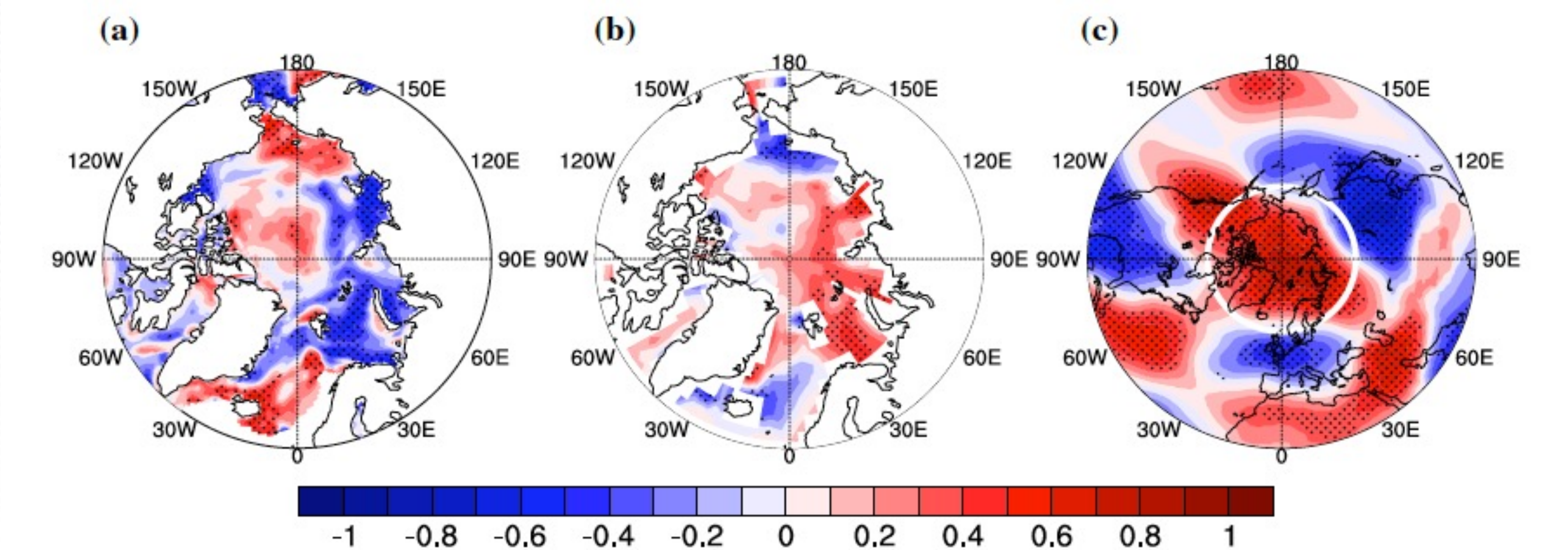

At the peak of the accumulative solar irradiance (i.e., 4 years after the maximum solar irradiance), the **JJAS mean Arctic sea ice concentration (a)** reaches a minimum over the Barents–Kara Sea region accompanied by an **Arctic sea surface warming (b)**, which then persists into the following winter, causing Arctic high-pressure extend to the Ural mountain region **(c, DJF mean 500-hPa geopotential)**, which enhances Siberian High and causes a bitter winter over the northern Asia.

Result 6: Influences from volcanic eruptions on ENSO and monsoon

1. A La Niña-like state in the second year after volcanic eruptions

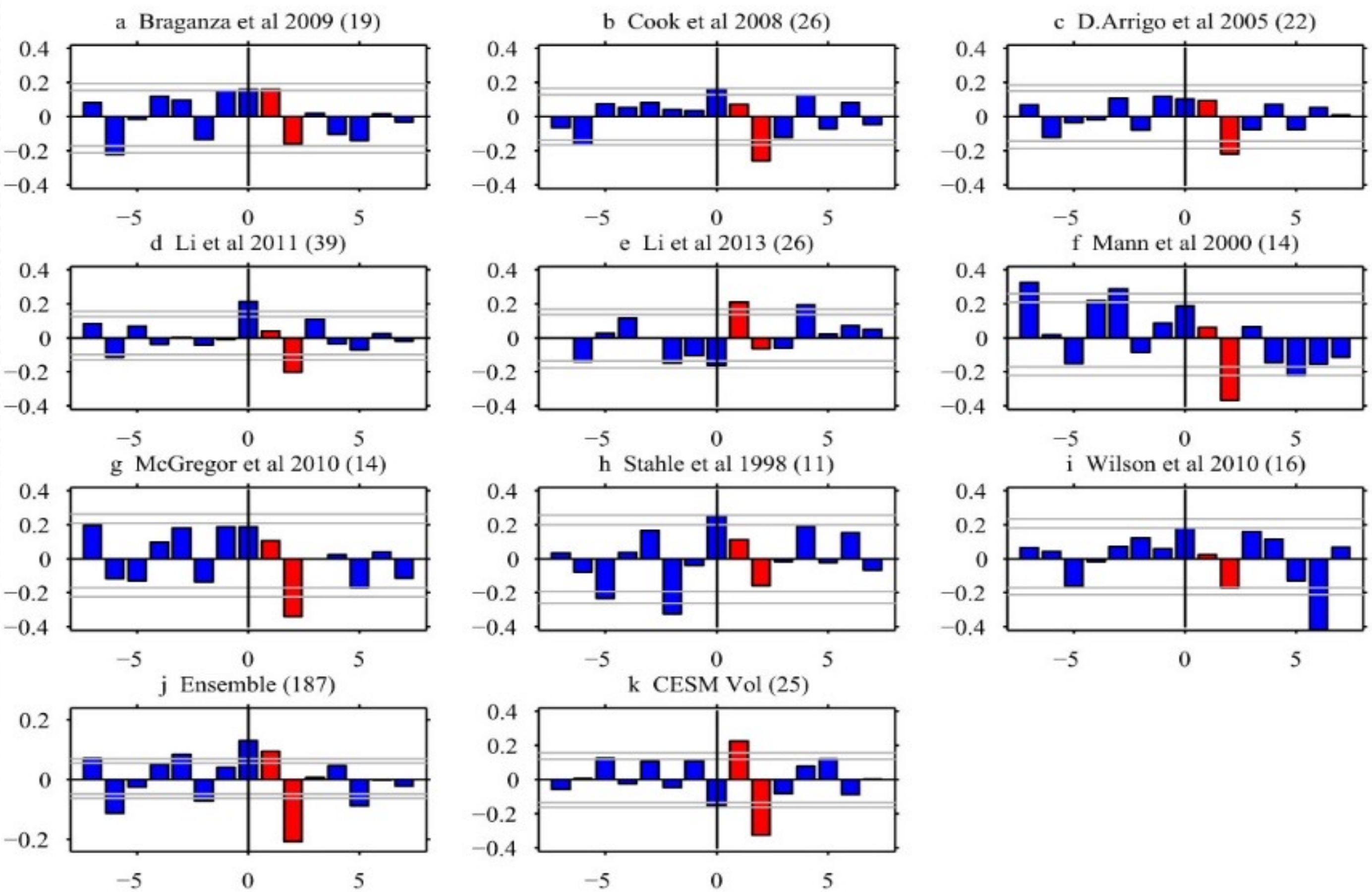

Shown in both reconstructions and model simulations, the El Niño-like states shift to the La Niña-like state in the second year after strong tropical volcanic eruptions, and then strong La Niña-like states occur during the winter of the third year.

(Sun et al., 2019, *Clim. Dyn.*)

Result 6: Influences from volcanic eruptions on ENSO and monsoon

1. A La Niña-like state in the second year after volcanic eruptions

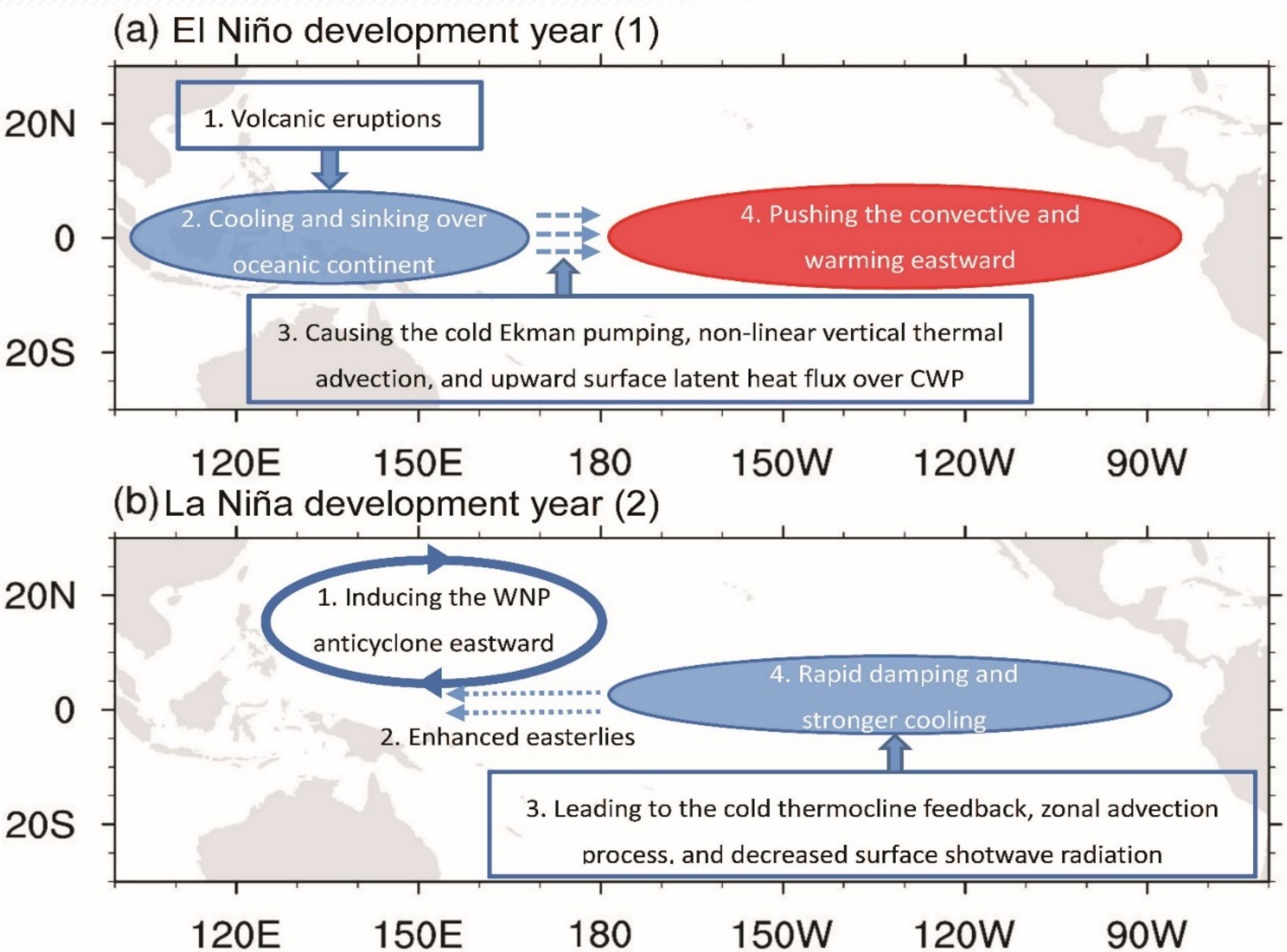

The **position of the anomalous WNPAC** established early in year (2) is **shifted eastward** under volcanic forcing, which is important for the rapid transition to La Niña

(Sun et al., 2019, *Clim. Dyn.*)

Result 6: Influences from volcanic eruptions on ENSO and monsoon

2. How northern high-latitude volcanic eruptions in different seasons affect ENSO

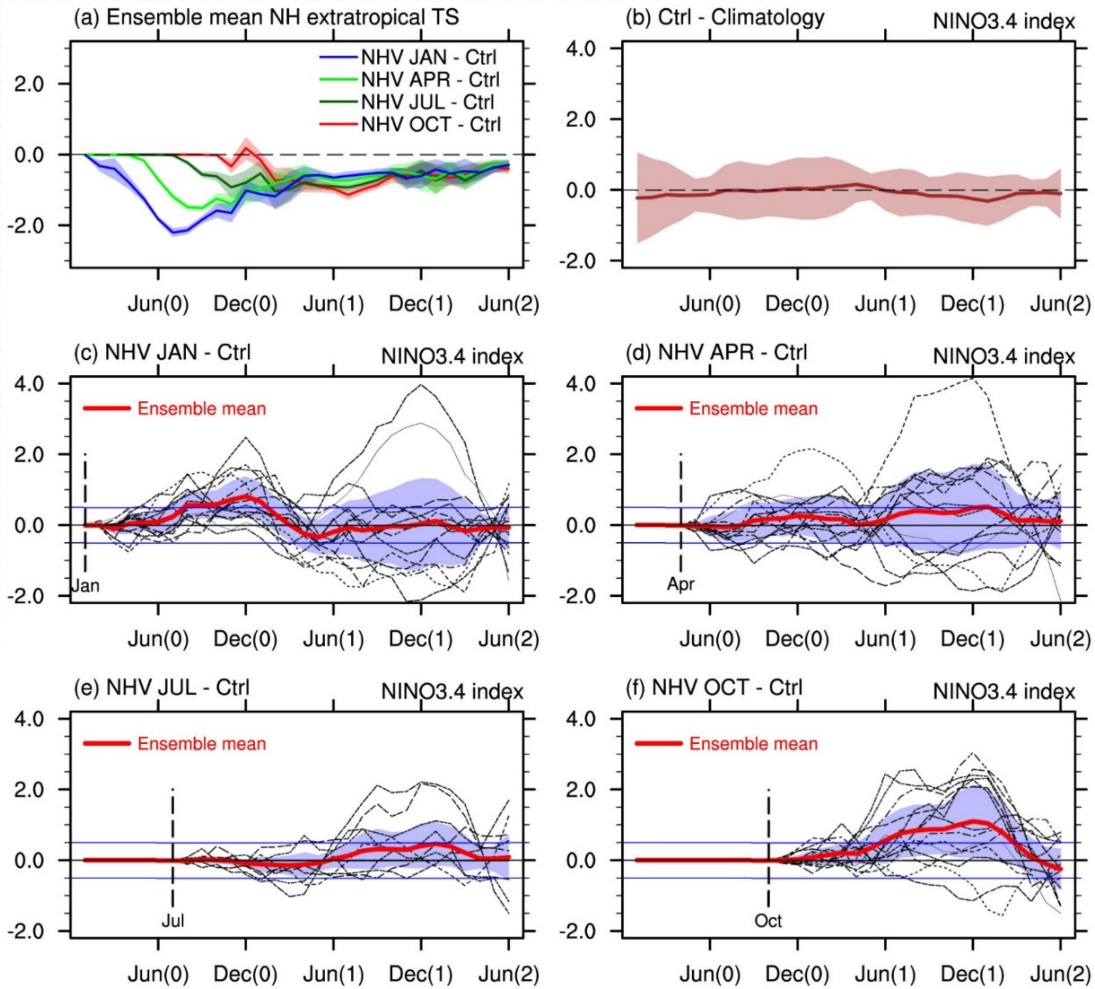

(a) simulated anomalous NH extratropical surface temperature. (b) Ensemble mean anomalies in Ctrl. (c)-(f) Anomalies in the JAN, APR, JUL and OCT experiments

The January eruption causes an El Niño in eruption year 0, while an El Niño occurs in year 1 after the October eruption.

No El Niño occurs after the April (July) eruption.

(Sun et al. 2019, *J. Climate*)

Result 6: Influences from volcanic eruptions on ENSO and monsoon

2. How northern high-latitude volcanic eruptions in different seasons affect ENSO

JAN experiment

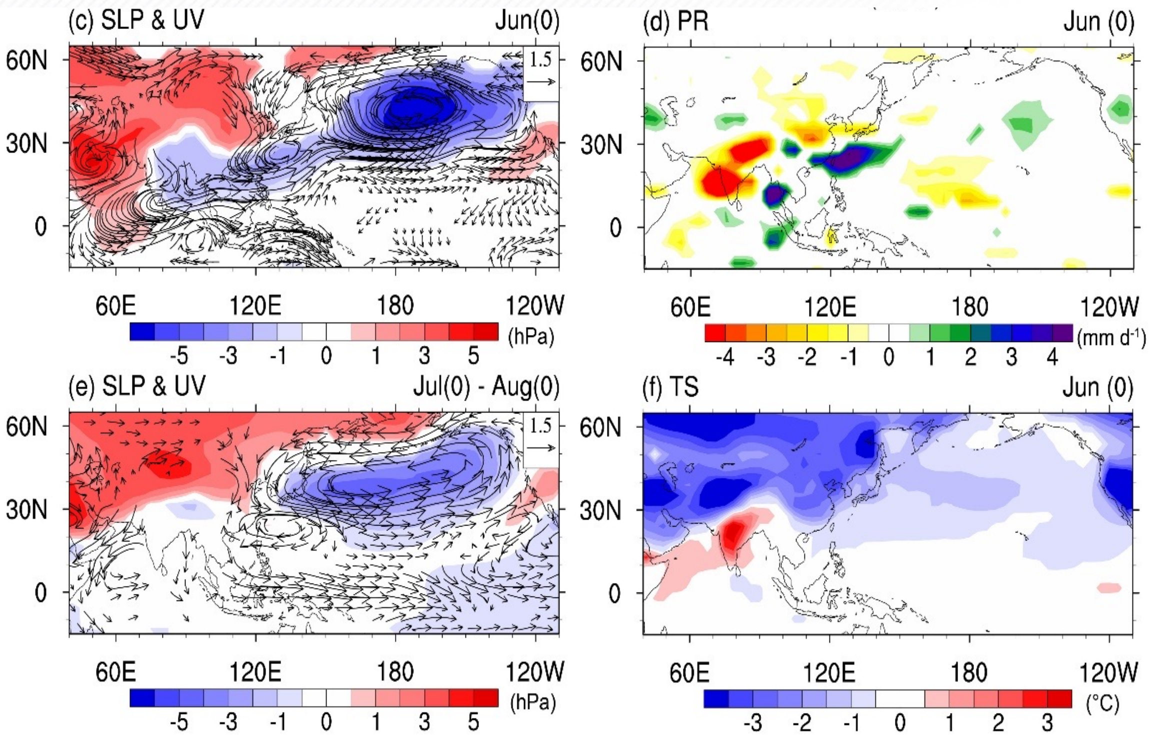

OCT experiment

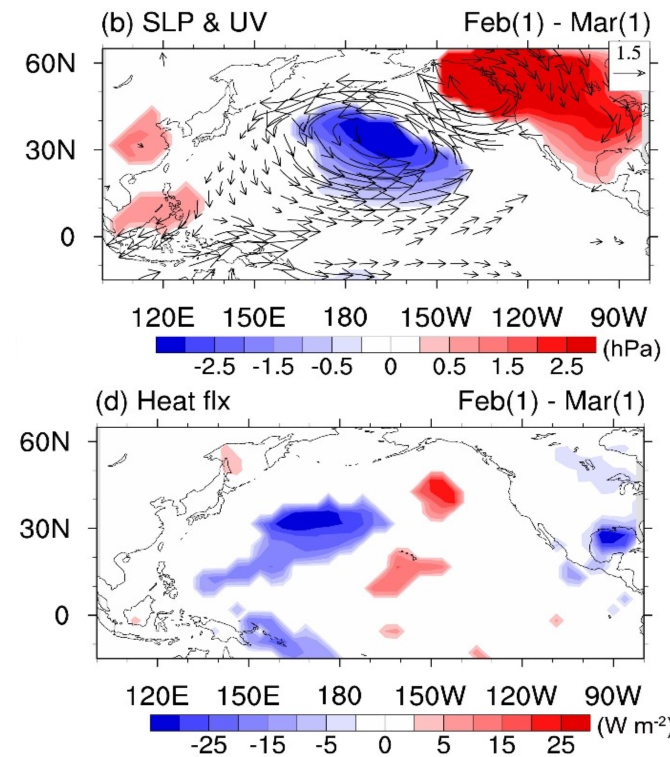

Anomalous North Pacific Cyclone (NPC) and Asian monsoon are key systems to excite anomalous westerlies, which is caused by the NHV-induced **mid-latitude cooling** and **Eurasian continent-North Pacific thermal contrast**.

(Sun et al. 2019, *J. Climate*)

3. Responses of polar regions to mega volcanic eruption

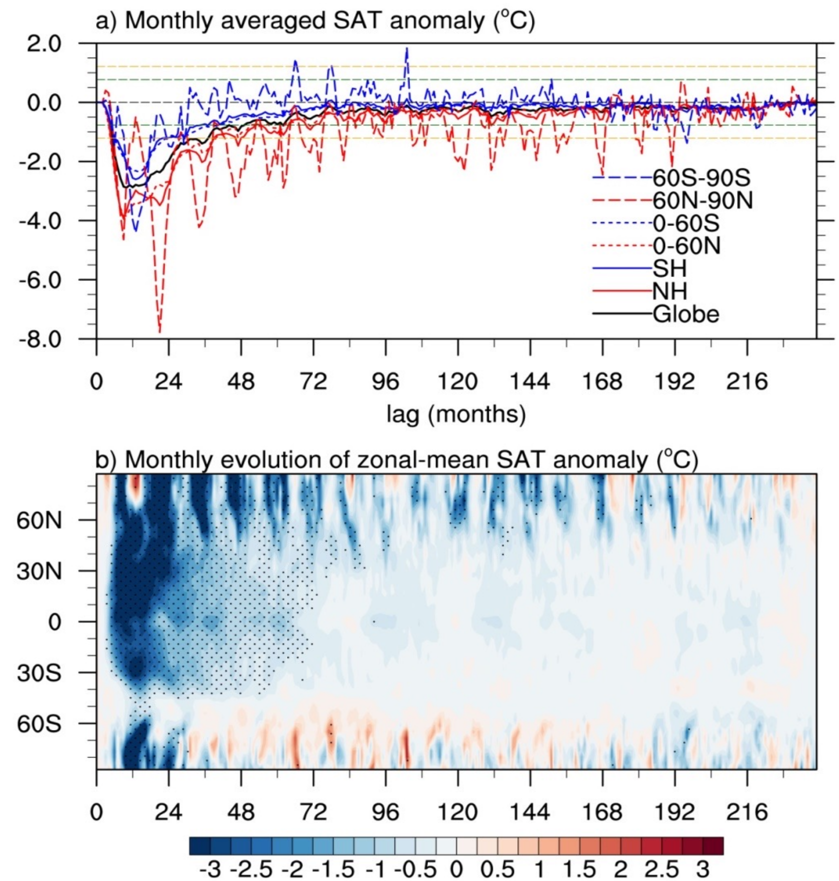

Remarkable asymmetry of temperature variation and duration between the Arctic and Antarctic.
A significant cooling in the Arctic for 16 years, while the cooling in the Antarctic lasted only 2 years.

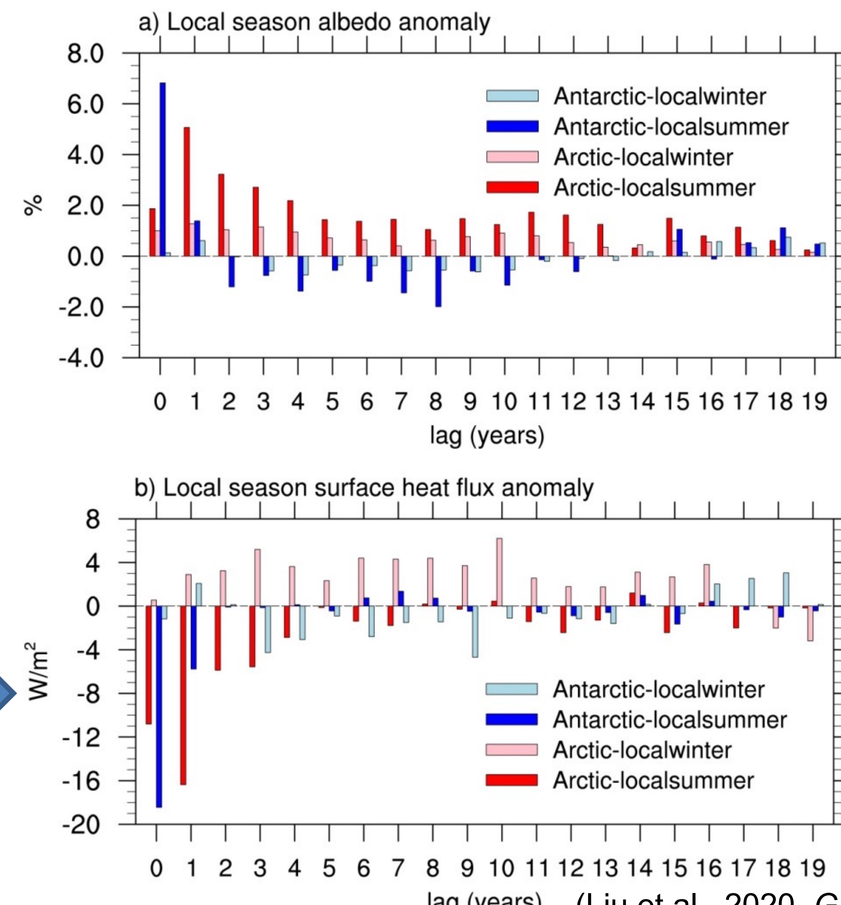

(Liu et al., 2020, *GRL*)

After a single mega volcanic eruption (such as Samalas), the combined effects of albedo feedback and ocean-atmosphere heat exchange related to sea ice changes are the main influencing factors for long-term asymmetric temperature changes in the Arctic and Antarctic.

Concluding remarks

- **A new group of experiments based on CESM covering the Holocene (NNU-Holocene) are designed to investigate the different influences on multi-scale climate variability from the natural forcings and anthropogenic forcings.**
- **Combined with the simulations covering last two millennia (NNU-2ka), TraCE-21ka, CESM-LME, etc., major conclusion are drawn:**
- **On Millennial scale:**
  - Green Sahara during mid-Holocene increases Northern Hemisphere land monsoon precipitation.
  - Middle East climate shifted from wet to dry due to the Saharan vegetation collapse during the mid-Holocene
- **On centennial scale:**
  - LUCC induce decreasing trend to the surface temperature.
  - 4.2 ka BP event may be induced by multi-century-scale internal variability, superimposed on the steady decline in SSTs and a reduction in the AMOC led by long-term changes of orbital forcing.

Concluding remarks

- **On multi-decadal scale:**
  - Volcanic forcing tends to reduce the megadrought frequencies through a negative PDO-like SSTA pattern, with larger SSTA over the eastern North Pacific than over the central North Pacific.
  - Ming Dynasty Megadrought is a typical drought triggered by internal variability and strengthened by the volcanic eruption, and this intensification is stronger during the late stage of droughts.
  - The 11-year insolation cycle has strong influences on decadal variations of the EASM and EAWM.
- **On interannual scale:**
  - Strong volcanic eruptions can induce fast shift from El Niño state to La Niña state in three years after eruptions.
  - Northern high-latitude volcanic eruptions in different seasons have different influences on ENSO.
  - Mega volcanic eruption induces a remarkable asymmetry of temperature variation and duration between the Arctic and Antarctic.

Publications since 2017

(1) Xue, J., L. Ning*, Y. Qin, K. Chen, M. Yan, and J. Liu, 2020: Comparisons on characteristics and mechanisms of the decadal megadroughts over eastern China between MCA and LIA. Int. J. Climatology, doi:10.1002/joc.6942 (online).

(2) Wang, Q., M. Yan*, J. Liu, L. Ning, 2020: Impacts of Land Use/Cover Change on Spatial Patterns of Summer Precipitation at Decadal Scale over Eastern China. Int. J. Climatology, doi:10.1002/joc.6939 (online)

(3) Yan, M., Z. Liu, L. Ning, and J. Liu, 2020: Holocene EASM-EAWM relationship across different timescales in CCSM3. Geophys. Res. Lett. 47, e2020GL088451, doi:10.1029/2020GL088451

(4) Liu, B., B. Wang, J. Liu, D. Chen, L. Ning, M. Yan, W. Sun, and K. Chen, 2020: Global and polar region temperature change induced by single mega volcanic eruption based on CESM simulation. Geophys. Res. Lett., 47, e2020GL089416, https://doi.org/10/1029/2020GL089416.

(5) Ning, L., K. Chen, J. Liu, Z. Liu, M. Yan, W. Sun, C. Jin, and Z. Shi, 2020: How do the volcanic eruptions influence the decadal megadrought over the eastern China? J. Climate, 33, 8195-8207.

(6) Chen, K., L. Ning*, Z. Liu*, J. Liu, M. Yan, W. Sun, L. Yuan, G. Lv, L. Li, Z. Shi, and C. Jin, 2020a: One drought and one volcanic eruption influenced the history of China: The Ming Dynasty Megadrought. Geophys. Res. Lett., 47, e2020GL088124, https://doi.org/10/1029/2020GL088124. (Nature research highlight)

(7) Yan, M., J. Liu, Z. Wang, and L. Ning, 2020: Biogeophysical impacts of land-use/land-cover change on 20th century anthropogenic climate compared to the impacts of greenhouse-gases change. Int. J. Climatology, 40(15), 6560-6573, DOI: 10.1002/joc.6598

(8) Chen, K., L. Ning*, Z. Liu, J. Liu, W. Sun, M. Yan, B. Liu, Y. Qin, and J. Xue, 2020: The influences of tropical volcanic eruptions with different magnitudes on persistent droughts over eastern China. Atmosphere, 11, 210, doi:10.3390/atmos11020210.

(9) Qin, Y., L. Ning*, K. Chen, J. Liu, and M. Yan, 2020: Assessment of PMIP3 model simulations of Megadroughts over the Eastern China during the Last Millennium. Int. J. Climatology, 40(12), 5188-5207

(10) Ning, L., J. Liu*, R. S. Bradley, M. Yan, K. Chen, W. Sun, and C. Jin, 2020: Elevation-dependent cooling caused by volcanic eruptions during last millennium. Int. J. Climatology, 40, 3142-3149, DOI: 10.1002/joc.6387.

(11) Chen, K., L. Ning*, W. Sun, Y. Qin, J. Xue, J. Liu, and M. Yan, 2020: Analyses of the characteristics and causes of Arctic Oscillation variability during the typical periods in last Millennium based on PMIP3 and CMIP5 simulations. Climatic and Environmental Research, 25(4), 429-442, doi:10.3878/j.issn.1006-9585.2019.19000 (in Chinese with English abstract)

(12) He, P., J. Liu, B. Liu, L. Ning, and M. Yan, 2019: Comparison of changes of Northern Hemisphere monsoon precipitation between two typical abrupt climate events in Holocene. Quaternary Sciences, 39(6): 1372-1383 (in Chinese with English abstract)

(13) Qiu, Y., J. Liu, B. Liu, L. Ning, and M. Yan, 2019: Characteristics of Holocene cold events in the Northern Hemisphere from the TraCE-21ka model simulation. Quaternary Sciences, 39(4): 1055-1067 (in Chinese with English abstract)

(14) Sun, W., B. Wang, Q. Zhang, F. S. R. Pausata, D. Chen, G. Lv, M. Yan, L. Ning, and J. Liu*, 2019: Northern Hemisphere land monsoon precipitation increased by the green Sahara during middle Holocene. Geophys. Res. Lett., 46, 9870-9879, doi: 10.1029/2019GL082116

(15) Jin, C., J. Liu*, B. Wang, L. Ning, and M. Yan, 2019: Decadal variability of northern Asian winter monsoon shaped by the 11-year solar Cycle. Clim. Dyn., 53, 6559-6568, DOI 10.1007/s00382-019-04945-4

Publications since 2017

(16) Jin, C., J. Liu*, B. Wang, M. Yan, and L. Ning, 2019: Decadal Variations of the East Asian Summer Monsoon Forced by the 11-Year Insolation Cycle. J. Climate, 32(10), 1735-1745. https://doi.org/10.1175/JCLI-D-18-0288.1

(17) Sun, W., B. Wang, J. Liu*, D. Chen, C. Gao, L. Ning, and L. Chen, 2019: How northern high-latitude volcanic eruptions in different seasons affect ENSO? J. Climate, 32, 3245-3262.

(18) Sun, W., J. Liu*, B. Wang, D. Chen, F. Liu, Z. Wang, L. Ning, and M Chen, 2019: A "La Niña-like" state occurring in the second year after large tropical volcanic eruptions during the past 1500 years. Clim. Dyn., 52(12), 7494-9509, doi:10.1007/s00382-018-4163-x

(19) Ning, L., J. Liu*, B. Wang, K. Chen, M. Yan, C. Jin, and Q. Wang, 2019: Variability and mechanisms of megadroughts over eastern China during the last millennium: A model study. Atmosphere, 10, 7, doi:10.3390/atmos10010007.

(20) Ning, L., J. Liu*, R. S. Bradley, and M. Yan, 2019: Comparing the spatial patterns of climate change in the 9th and 5th millennia B.P. from TRACE-21 model simulations. Climate of the Past, 15, 41-52, doi:10.5194/cp-15-41-2019

(21) Liu, L., T. Zhou, L. Ning*, J. Liu, M. Yan, C. Jin, and W. Sun, 2019: Linkage between the Arctic Oscillation and summer climate extreme events over the middle reaches of Yangtze River Valley. Climate Research, 78, 237-247, doi: 10.3554/cr01542

(22) Liu, L., L. Ning*, J. Liu, M. Yan, and W. Sun 2019: Prediction of Summer Extreme Precipitation over the Middle and Lower Reaches of the Yangtze River Basin, Int. J. Climatology, 39, 375-383, doi: 10.1002/joc.5813

(23) Yan, M., B. Wang, J. Liu*, A. Zhu, L. Ning, and J. Cao, 2018: Understanding the Australian Monsoon change during the Last Glacial Maximum with a multi-model ensemble. Climate of the Past, 14, 2037-2052, doi:10.5194/cp-14-2047-2018

(24) Ning, L., J. Liu*, Z. Wang, and R. S. Bradley, 2018: Different influences on the tropical Pacific SST gradient from natural forcing and anthropogenic forcing. Int. J. Climatology, 38, 2015-2028, doi:10.1002/joc.5313.

(25) Ning, L., J. Liu*, and B. Wang, 2017: How does South Asian High influence extreme precipitation over eastern China? J. Geophys. Res. Atmos., 122, 4281-4298, doi:10.1002/2016JD026075

(26) Ning, L., J. Liu*, and W. Sun, 2017: Influences of volcano eruptions on Asian Summer Monsoon over the last 110 years. Scientific Reports, 7, 42626, doi:10.1038/srep42626

(27) Jin C., Liu J*., Wang B. et al. A Centennial Episode of Weak East Asian Summer Monsoon in the Midst of the Medieval Warming[J]. Paleoceangraphy and Paleoclimatology, 2018, 33(9):1035-1048.

(28) Yan, M., and J. Liu*, 2019: Physical processes of cooling and mega-drought during the 4.2 ka BP event: results from TraCE-21ka simulations. Climate of the Past, 15, 265-277

(29) Wan L., Liu Z*., Liu J*. et al. On the linearity of the temperature response in Holocene: the spatial and temporal dependence. Climate of the Past, 2019, 15, 1411-1425

(30) Sun W., B. Wang, D. Chen, C. Gao, G. Lv, and J. Liu, 2021: Global monsoon response to tropical and Arctic stratospheric aerosol injection. Climate Dynamics, doi:10.1007/s00382-020-05371-7. (accepted)

Thank you!

For comments and questions, please contact: ningliangnnu@njnu.edu.cn

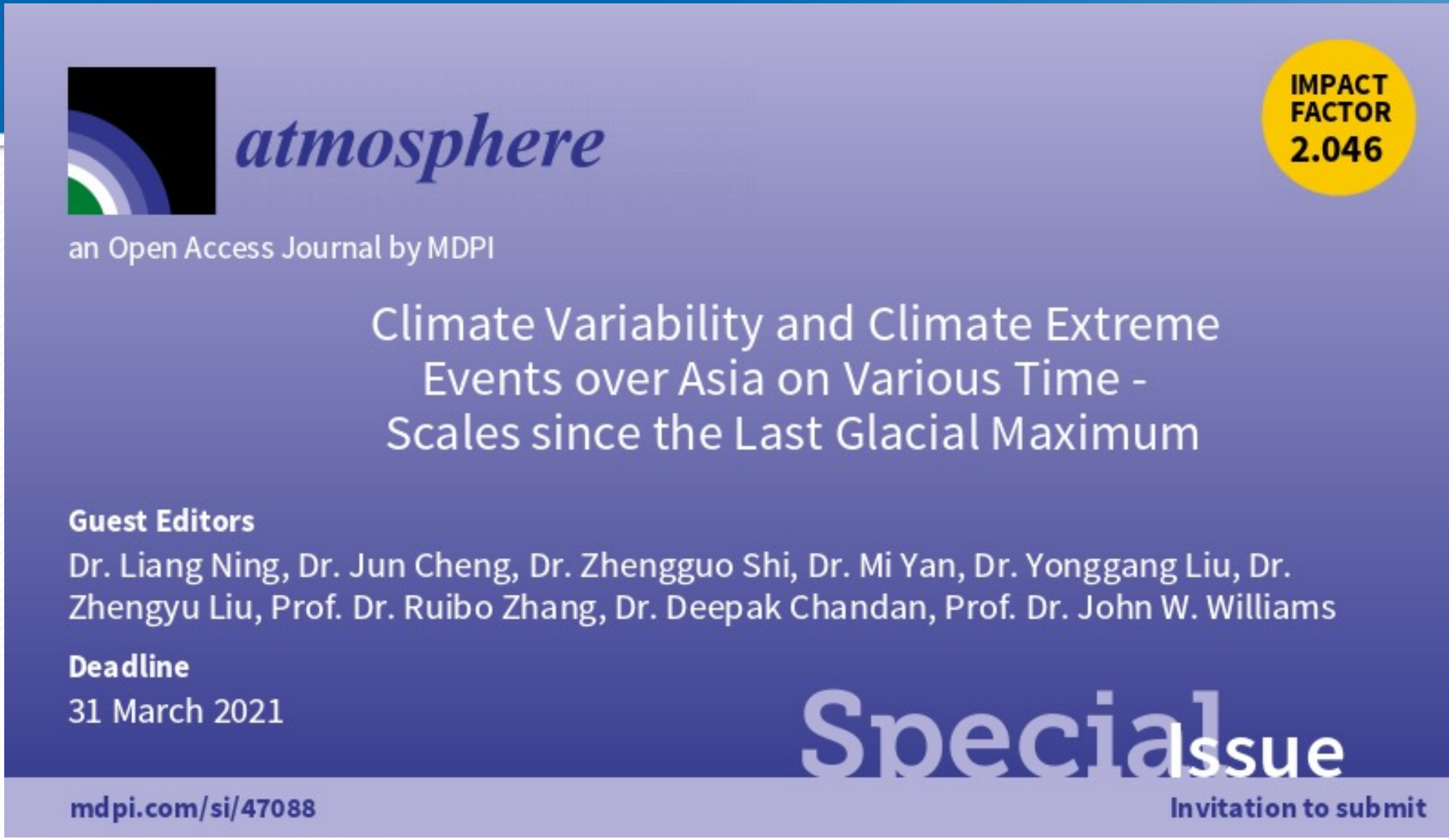

Special Issue at *Atmosphere* (*IF*=2.046): Climate variability and climate extreme events over Asia on various time scales since the Last Glacial Maximum
Deadline: 31 March, 2021